Insight of the metal-ligand interaction in f elements complexes by paramagnetic NMR spectroscopy

M. Autillo, L. Guerin, T. Dumas, M. S. Grigoriev, A. M. Fedoseev, S. Cammelli, Pl. Solari, D. Guillaumont, P. Guilbaud, P. Moisy, et al.

▶ **To cite this version:**

M. Autillo, L. Guerin, T. Dumas, M. S. Grigoriev, A. M. Fedoseev, et al.. Insight of the metal-ligand interaction in f elements complexes by paramagnetic NMR spectroscopy. Chemistry - A European Journal, 2019, 25 (17), pp.4435 -4451. 10.1002/chem.201805858 . cea-02339876

HAL Id: cea-02339876

https://cea.hal.science/cea-02339876

Submitted on 5 Nov 2019

HAL is a multi-disciplinary open access archive for the deposit and dissemination of scientific research documents, whether they are published or not. The documents may come from teaching and research institutions in France or abroad, or from public or private research centers.

L'archive ouverte pluridisciplinaire **HAL**, est destinée au dépôt et à la diffusion de documents scientifiques de niveau recherche, publiés ou non, émanant des établissements d'enseignement et de recherche français ou étrangers, des laboratoires publics ou privés.

Insight of the metal-ligand interaction in f elements complexes by paramagnetic NMR spectroscopy

Matthieu Autillo,[a] Laetitia Guerin,[a] Thomas Dumas,[a] Mikhail S. Grigoriev,[d] Alexandre M. Fedoseev,[d] Sebastiano Cammelli,[c] Pier Lorenzo Solari,[c] Dominique Guillaumont,[a] Philippe Guilbaud,[a] Philippe Moisy,[a] Hélène Bolvin,*[b] and Claude Berthon*[a]

Abstract: The magnetic properties of Ln(III) and An(III) complexes formed with dipicolinate ligands have been studied by NMR spectroscopy. To know precisely the geometry of these complexes, a crystallographic study by single-crystal X-Ray Diffraction (XRD) and by Extended X-Ray Absorption Fine Structure (EXAFS) in solution was performed. Several separation methods of paramagnetic shifts observed on the NMR spectra were applied to these complexes. Methods using several nuclei of the dipicolinate ligands revealed an abrupt change in the geometry of the complexes and a metal-ligand interaction in the middle of the lanthanide series. The study of paramagnetic shifts with temperature demonstrated that higher order terms in the dipolar and contact contributions are required especially for the lightest Ln(III) cations and almost all studied An(III). The Bleaney's parameters $\langle S_z \rangle_a$ and C_a^D related to the contact and dipolar terms respectively were deduced from experimental data and compared to *ab-initio* calculations. A quite good agreement is found for $\langle S_z \rangle_a$ and C_a^D temperature dependences. However C_a^D values obtained from cation magnetic anisotropy calculations lead to some differences with Bleaney equations defined for Ln(III). Other parameters such the crystal field parameter and the hyperfine constants F_i obtained from experimental data with $[An(ethyl\text{-}DPA)_3]^{3-}$ complexes are at odds with assumptions underlying Bleaney's theory.

1. Introduction

The chemistry of actinide elements in solution has been the subject of many studies, particularly in order to understand the behavior difference between actinides and lanthanide elements in oxidation state +III (noted An(III) and Ln(III) respectively). These researches, carried out as part of nuclear fuel recycling, have led to attribute this difference to a higher covalent character in the actinide complex formation.[1] Despite numerous efforts to prove and quantify this phenomenon, it remains difficult to clearly interpret the chemical properties of these elements in solution. The study of the actinides paramagnetic behavior can be a "simple" method to analyze their electronic properties and to obtain information on the ligand-actinide interaction.

The paramagnetic properties of Ln(III) cations have been extensively studied by NMR spectroscopy.[2] The presence of a paramagnetic ion in a coordination complex induces an additional chemical shifts and line broadening. This feature depends both on the nature of the paramagnetic element and on the observed nucleus by NMR. The induced chemical shift is exploited to perform structural analysis of Ln(III) complexes so that the paramagnetic element is also known as paramagnetic probe.[2b, 3] The experimental chemical shift $(\Delta_{tot})_{i,a}$ for the observed nucleus i of a ligand in a complex with a lanthanide a arises from three independent contributions: i) a contribution related to the sample magnetic susceptibility $(\delta_{bulk})_a$, ii) a diamagnetic contribution $(\delta_{dia})_{i,a}$ and iii) a paramagnetic contribution $(\delta_{para})_{i,a}$ and therefore it can be written as:

$$(\Delta_{tot})_{i,a} = (\delta_{bulk})_a + (\delta_{dia})_{i,a} + (\delta_{para})_{i,a} \quad (1)$$

The contribution due to the sample magnetic susceptibility $(\delta_{bulk})_a$ affects all nuclei in an identical manner and is usually overcome by introducing an internal reference in the medium for which the characteristic signal undergoes a similar shift to the studied complex.

The diamagnetic contribution $(\delta_{dia})_{i,a}$ arises from the redistribution of the electron density within the ligand after the complexation with Ln(III) ion. It is generally low compared to the paramagnetic shifts and can be considered negligible in many cases with the exception of close or directly linked nuclei to the Ln(III) ion.[4] However, this component can be easily estimated by measuring the experimental chemical shift of a nucleus i for an isostructural diamagnetic complex. In the case of lanthanide complexes, analogs compounds of La(III) or Lu(III) will be used assuming that this term is identical for all the other lanthanides. This assumption seems reasonable because the chemical shifts induced by lanthanum (lightest) and lutetium (heaviest) are generally very similar.[5] For the An(III) cations, isostructural compounds of La(III) and Lu(III) will be also used to overcome the unfeasibility to analyze Ac(III) complexes.

The paramagnetic contribution $(\delta_{para})_{i,a}$ is due to the interaction between the electronic magnetic moment of the metal center a and the nuclear spins i of the ligand. It is the sum of two components:

[a] Dr M. Autillo, L. Guerin, Dr. T. Dumas, Dr. P. Guilbaud, Dr. C. Berthon, Dr. P. Moisy
CEA, Nuclear Energy Division, Research Department of Mining and Fuel Recycling Processes, BP 17171, F-30207 Bagnols sur Cèze, France
E-mail: claude.berthon@cea.fr

[b] Dr. H. Bolvin
Laboratoire de Physique et de Chimie Quantiques
Université Toulouse 3, 118 Route de Narbonne, 31062 Toulouse, France.
E-mail: bolvin@irsamc.ups-tlse.fr

[c] S. Cammelli, P-L Solari
Synchrotron SOLEIL, L'orme des Merisiers, Saint Aubins, BP 48, F-91192, Gif sur Yvette cedex, France.

[d] M.S. Grigoriev, A.M. Fedoseev, A.N. Frumkin Institute of Physical Chemistry and Electrochemistry, Russian Academy of Sciences, Moscow, 119071, Russia.

Supporting information (SI) for this article is given via a link at the end of the document. It contains X-ray and EXAFS data for An^{3+}/Ln^{3+} complexes, ^1H and ^{13}C paramagnetic shifts, exploitation of ^1H and ^{13}C chemical shifts by one nucleus methods, of ^{13}C chemical shifts by the three nuclei method and paramagnetic shifts variation with temperature.

WILEY-VCH

- a contact component $(\delta_c)_{i,a}$ related to the delocalization of the spin density of the paramagnetic cation a towards the nucleus *i* through the chemical bond;

- a dipolar or pseudocontact component $(\delta_{pc})_{i,a}$ associated with the through-space dipolar interaction between the electronic and the nuclear magnetic moments of the paramagnetic center a and the nucleus *i*.

After subtracting the diamagnetic contribution and the contribution due to the sample magnetic susceptibility, the paramagnetic chemical shift $(\delta_{para})_{i,a}$ for a nucleus *i* and a lanthanide a can be expressed as:

$$\left(\delta_{para}\right)_{i,a} = (\Delta_{tot})_{i,a} - (\delta_{bulk})_a - (\delta_{dia})_{i,a} \quad (2)$$

$$\left(\delta_{para}\right)_{i,a} = \left(\delta_{pc}\right)_{i,a} + (\delta_c)_{i,a} \quad (3)$$

Then, components $(\delta_c)_{i,a}$ and $(\delta_{pc})_{i,a}$ may be expressed as the product of several terms related to the lanthanide ion a and the nucleus *i* according to the equation:

$$\left(\delta_{para}\right)_{i,a} = G_i A_2^0 < r^2 > C_a^D + F_i \langle Sz \rangle_a \quad (4)$$

where $A_2^0 < r^2 >$ is the axial ligand field parameter of 2nd order, C_a^D is a magnetic constant at a given temperature (also called dipolar coupling) which measures the axial magnetic anisotropy of a paramagnetic ion (a) (calculated by Bleaney for Ln^{3+}),[6] F_i is proportional to the electron-nucleus hyperfine coupling constant $A/_h = \gamma B_0 F_i$ (expressed in MHz) and $\langle Sz \rangle_a$ is the thermal average of the electron spin magnetization along the external magnetic field (calculated for Ln^{3+}).[7] Finally, G_i is the geometric factor of the nucleus of interest containing complex structural information. In the case of a cylindrical symmetry, it can be defined by the following equation:

$$G_i = \frac{3cos^2\theta_i - 1}{r_i^3} \quad (5)$$

where r_i is the Ln-nucleus *i* distance and θ_i is the angle between the Ln-nucleus *i* vector and the main axis of the magnetic susceptibility tensor.

Eq. (4) is based upon a series of assumptions made by Bleaney that have been scrutinized up until recently.[8] Within this approach, the magnetic moment of the unpaired electrons is approximated by a point dipole at the metal position, the magnetic anisotropy axis aligns along the main molecular C_n axis, the ligand field splitting is much less than kT (200 cm^{-1} at room temperature) and the contribution of ligand field at higher order terms are ignored. From these two latter assumptions, it comes out the total angular momentum of the cation J is implicitly supposed to be a good quantum number so that the Bleaney's constant C_a^D only depends on the cation a and not on the ligand. Since its application over more than 40 years, it is still difficult to find out why NMR studies with some lanthanides complexes are consistent with these simplifications[9] while others not[10] [11]. Albeit Bleaney's theory effectiveness could appear lower than recent quantum mechanical treatments[12] we have undertaken to evaluate to what extent the ligand field could skew the Bleaney's theory using An(III) instead of Ln(III) with 2,6-dipicolinic acid (DPA). Due to the larger radial extent of 5*f* orbitals than 4*f* ones, a larger covalence and ligand field effects are expected so that the applicability or validity of Bleaney's equation may be questioned. It also could be an opportunity to get a better insight on covalent behavior of An/Ln cations through Bleaney's parameters.

In order to determine the covalent part in the coordination bonds and to characterize three-dimensional structure of actinide complexes in solution, the major difficulty is to separate the two contributions $(\delta_c)_{i,a}$ and $(\delta_{pc})_{i,a}$ of the paramagnetic chemical shift $(\delta_{para})_{i,a}$. Various separation techniques have been evaluated by Reilley[3f] in 1976 for Ln(III) cations. Several methods consider either a pure dipolar or a pure contact[13] chemical shift while other ones exploit their temperature dependence.[3c, 3f] A more stringent method is to evaluate data for different Ln(III) across an isostructural series by using the tabulated lanthanide constants $\langle Sz \rangle_a$ and C_a^D.[3d, 3g, 3h, 5, 14] Unfortunately these constants do not exist for the An(III) series and it would be of interest to evaluate them. By comparing with those of the Ln series these parameters could be relevant as a covalency scale, assuming the Bleaney's theory still applicable.

In this work, several methods are applied to the study of Ln(III) and An(III) complexes with ethyl-DPA ligand (Scheme 1). This ligand provides more ^{13}C and ^{1}H NMR signals far from the paramagnetic center than the commercial DPA. However the ethyl group is flexible, so structural information gained from XRD at solid state would not be representative from NMR conformations in liquid state. For this reason XRD studies were performed on Ln(III) and An(III) DPA ligand.

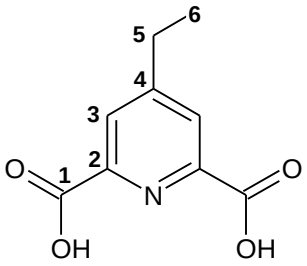

Scheme 1. Ethyl-DPA ligand (4-ethyl-2,6-dipicolinic acid).

Like the Ln(III), An(III) ions form stable 1:3 complexes with the DPA ligand leading to rigid structures in solution. Thus, these An(III) compounds can be isolated and their structure determined by XRD in solid state and EXAFS in solution. This ensures the structural information from solid state is proper for NMR analysis in solution. A complete crystallographic study has been first performed and we have secondly checked the structure is kept the same along the series. Then, based on several separation methods of experimental data and the contribution of quantum chemical calculations, terms only depending on the An(III) cations in the Eq. (4) have been determined and discussed.

2. Results and Discussion

2.1. Structural study

In solid state, the compounds $Ln/An(DPA)_3(C_3H_5N_2)_3 \cdot 3H_2O$ (Ln = La - Lu and An = Pu, Am) are isostructural along the series and crystallize in a triclinic space group $P\bar{1}$ (refer to SI and cif files). The coordination sphere contains three DPA ligands forming a tricapped trigonal distorted prism. Each ligand is tridentate and coordinated to the Ln(III) / An(III) cation by the nitrogen atom of the pyridine cycle (capped position) and the two

oxygen atoms of the carboxylate groups (prism position). The charge compensation of the anionic complexes is provided by three imidazolium cations and three water molecules are included into the structure (crystallographic data and structure determination details are given in **Table S8**).

Since the Ln(III) and An(III) complexes are isostructural with a coordination number of 9, one may analyze the influence of the 4*f*/5*f* orbitals in the bonding between the metal ion and the ligands. First, Ln/An - O and Ln/An - N bond lengths decrease along the lanthanide and actinide series accordingly to the decrease in ionic radius (**Figure 1**). It is noteworthy that Am(III) - N and Am(III) - O distances found in literature for DPA compounds are in agreement with our X-ray results.[15] While the curves for An(III) - O and Ln(III) - O place on the top of each other the curve for An(III) - N lies below than for Ln(III) - N. Hence nitrogenous bonds are more sensitive to An/Ln differences than the carboxylate group. For a given ionic radius, the shorter the distance the more covalent character the bond is. This has already been observed in other series of isostructural complexes.[16] This observation is often attributed to a larger degree of covalence for the actinide cations and related to ligand selectivity.

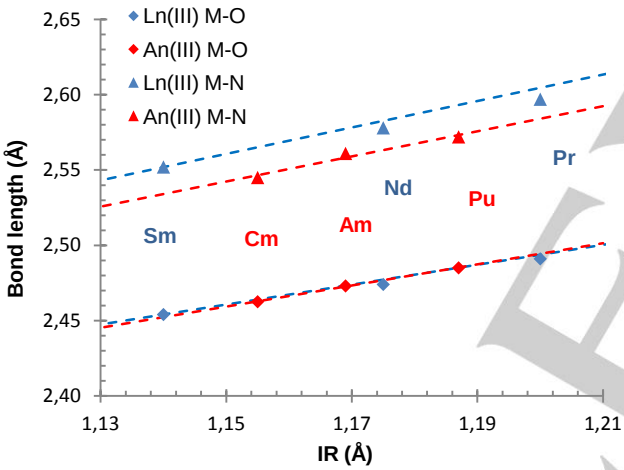

Figure 1: Bond length M – O and M – N of the coordinating atoms in $M(DPA)_3(C_3H_5N_2)_3 \cdot 3H_2O$ versus the ionic radius for M=Pu(III), Am(III) from this work and from Cary *et al.* [15] for Cm(III). The ionic radii have been determined by D'Angelo *et al.* for Ln(III) cations[17] and by David *et al.* for An(III) cations.[18]

EXAFS spectra were recorded at the L_{III} edge of Pr(III), Dy(III) and Yb(III) to ensure the crystallographic structure conservation (stoichiometry and bond length in the coordination sphere) along the series of the dipicolinate complexes in solution (DMSO). The spectra and the corresponding Fourier transforms are presented in Supporting Information (SI hereafter). The diffusion paths have been calculated with the FEFF program[19] from the crystallographic data of $Ln(DPA)_3(C_3H_5N_2)_3 \cdot 3H_2O$ compounds. The parameters of the experimental spectra adjustment procedure, described in experimental section are presented in SI. The Fourier transform shows a dominant peak from the contribution of oxygen (O_I) and nitrogen (N) of the first coordination sphere followed by three peaks of lower amplitude corresponding to successively carbon atoms of carboxylate group (C_I), pyridine ring (C_{II}) and the second oxygen atom of the carboxylate group (O_{II}) (**Figure 2**). By comparing the results obtained by monocrystal XRD and EXAFS fitting, we confirm that the structure of Ln(III) complexes is stable in DMSO solution. Based on these results, it can be considered that the crystallographic structure of the $An(ethyl\text{-}DPA)_3^{3-}$ complexes is maintained in solution. To confirm this hypothesis, this study was extended to the actinide elements. However, for plutonium(III), a rapid oxidation occurs under X-ray measurements. The acquisition of statistically satisfactory EXAFS data has therefore been carried out on Am(III) complex. The EXAFS spectrum obtained at L_{III} edge of americium and the corresponding Fourier transform are shown in **Figure 2**. The simple and scattering paths have been calculated on the basis of the crystallographic data of $Am(DPA)_3(C_3H_5N_2)_3 \cdot 3H_2O$ compound and parameters of the spectra adjustment procedure are summarized in SI with comparison to XRD metric parameters.

The agreement between the X-ray crystallographic and EXAFS results in DMSO solution validates the use of the crystallographic structure of Ln(III) and An(III) complexes to calculate the structural parameters.

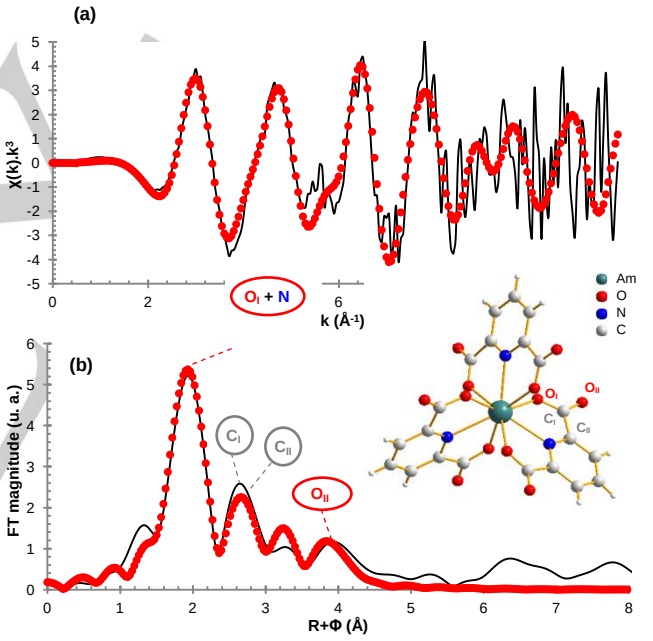

Figure 2. EXAFS experimental (solid line) spectra of $[Am(ethyl\text{-}DPA)_3]^{3-}$ in solution (a) and the corresponding Fourier transform (b). The best fit is represented with red circles.

No crystal structures are available for $[Ln/An(ethyl\text{-}DPA)_3]^{3-}$ complexes and structural information on the ethyl chain nuclei of the ligand are not available. As mentioned above, the ethyl chain is highly moveable in solution and the crystalline organization of a solid compound would not be representative of these movements. To approach an average position of the ligand in solution, a sampling of ethyl chain positions was performed by Molecular Dynamics (MD) calculations based on the crystal structures of $Ln/An(DPA)_3(C_3H_5N_2)_3 \cdot 3H_2O$: The Ln(III) and An(III) cations surrounded by the DPA ligand were kept motionless all along the simulation in agreement with the XRD and EXAFS first shell structure. Only the ethyl chain was considered mobile in order to extract structural information (θ and r, see Eq (5))

averaged over 5000 snapshots from MD trajectories. Regarding Cm(III) and Cf(III) complexes of ethyl-DPA, MD calculations were performed from published An(HDPA)$_3$•H$_2$O XRD data[15]. Λ and Δ enantiomers lead to very similar structural parameters (see **Table S5**). As Cary *et al*. mentioned we observed that co-crystallized water molecules induce distortions for one of the three DPA into the enantiomers. Strained DPA were excluded from G_i calculations.

2.2. ^{1}H and ^{13}C paramagnetic shift study

^{1}H and ^{13}C NMR spectra of [Ln/An(ethyl-DPA)$_3$]$^{3-}$ were obtained in DMSO-d6 solution. The paramagnetic induced shift of Ln(III) and An(III) cations were deduced using the complex [La(ethyl-DPA)$_3$]$^{3-}$ as diamagnetic reference. A summary of the chemical shift values are given in SI (**Table S2**) at room temperature. The ^{13}C signals of the Cm(III) complex were not observed due to the important line broadening induced by this cation associated with the low radioactive element concentration.

The different methods commonly used with Ln(III) complexes to separate the contact and dipolar contributions have been applied to An(III) compounds. Isostructurality, field ligand and hyperfine coupling constancy along Ln(III) and An(III) cation series are valuable information that can be deduced. Bleaney's constants $\langle Sz \rangle_a$ and C_a^D will be deduced hereafter from temperature experiments.

Paramagnetic shift vs. geometric term:

For the ^{1}H NMR spectra of organic molecules, shifts induced by paramagnetic lanthanides are generally assigned to the dipolar interaction with the exception of aromatic systems.[2a] For this reason, contact contributions are expected in the proton chemical shifts of the ethyl-DPA owing to the pyridine cycle. Nevertheless, protons of the ethyl group branched on the pyridine are far away from the paramagnetic center (5 bonds away) and then are assumed to have a negligible contact contribution. In this case, the 2nd term of Eq. (4) disappears and the ratio between the shifts of two ^{1}H nuclei (*i* and *j*) in the sample complex simplifies to the ratio of the geometrical factors:

$$\frac{(\delta_{para})_{i,a}}{(\delta_{para})_{j,a}} = \frac{G_i A_2^0 \langle r^2 \rangle C_a^D}{G_j A_2^0 \langle r^2 \rangle C_a^D} = \frac{G_i}{G_j} = R_{ij} \qquad (6)$$

Table 1 compares these ratio R_{ij} deduced from chemical shifts and from geometrical parameters for Ln(III) and An(III) ethyl-DPA complexes. Geometrical factors G_i/G_j are deduced from crystallographic data and molecular dynamic calculations while paramagnetic chemical shifts $(\delta_{para})_{i,a}/(\delta_{para})_{j,a}$ are obtained at 298K in DMSO-d6.

Table 1. Ratios of Eq. (6) between geometric factors deduced from structural data (H_3) and molecular dynamic calculations (H_5 and H_6) for La, Ce, ,Pr, Nd, Dy, Er, Yb, Pu and Am complexes), and between proton paramagnetic shifts at 298K of [Ln/An(ethyl-DPA)$_3$]$^{3-}$ complexes. Ratios are given for two pairs of protons H_3-H_6 and H_5-H_6 as labelled Scheme 1.

	G_{H_3}/G_{H_6}	$(\delta_{para})_{H_3}/(\delta_{para})_{H_6}$	G_{H_5}/G_{H_6}	$(\delta_{para})_{H_5}/(\delta_{para})_{H_6}$
Ce		2.4		1.0
Pr		2.5		0.9
Nd		3.8		-0.1
Sm		1.9		1.7
Eu		4.1		0.1
Tb	**2.16 ±0.01**	2.0	**1.27 ±0.01**	1.5
Dy		2.0		1.5
Ho		2.1		1.5
Er		2.5		1.1
Tm		2.3		1.3
Yb		2.3		1.3
Pu		18.0		26.7
Am	**2.11**	-5.2	**1.27 ±0.01**	-13.3
Cm	**±0.03**	2.2		1.5
Cf		-4.2		-9.3

The results obtained for the Ln(III) complexes are different along the series. First, for the first half of the series (from Ce(III) to Eu(III)), a significant difference between the geometric factors ratios and the chemical shifts ratios is observed. This suggests that a contact term appears up to six bonds from the paramagnetic center or that Eq. (4) does not properly describe the dipolar contribution. Conversely, a better agreement is found for the cations of the second part (from Tb(III) to Yb(III)) suggesting a low contact contribution. We can imagine that either a slight conformational change occurs in the middle of the Ln(III) series or that the increasing *J* (total angular momentum quantum number) value toward the end of the series makes the dipolar contribution greater and then less sensitive to the contact contribution.

Regarding An(III) cations, higher modifications are found between the calculated geometric and the experimental chemical shifts ratios. These deviations seem to show that a significant contact contribution is extended up to 6 bonds from the paramagnetic center for An(III) cations with An = Pu, Am and Cf. This can be related to a larger covalence which was otherwise observed through ^{15}N NMR experiments[20]. On the contrary, the experimental chemical shifts ratios are close to the theoretical ratios for Cm(III) pointing out the observed paramagnetic chemical shifts are mainly dipolar for this cation. Conversely to the Ln(III) series it can be noted that the paramagnetic shifts induced by the actinide cations do not monotonically vary with the cation-proton distance. For example, the largest chemical shift appears on the H_3 protons for Cm(III) while it appears on H_5 protons for the Pu(III), Am(III) and Cf(III) complexes (See **Table S2**).

To check whether observed deviations are not due to a geometric variation of the complexes in solution. an analysis method using the paramagnetic shifts of two nuclei *i* and *k* within the same metallic complex a has been proposed.[14b]

$$\frac{(\delta_{para})_{i,a}}{\langle S_z \rangle_a} = (F_i - R_{ik}F_k) + R_{ik}\frac{(\delta_{para})_{k,a}}{\langle S_z \rangle_a} \qquad (7)$$

This equation assumes the ligand field parameter constant along the cation series. R_{ik} , the ratio between G_i and G_k of nuclei *i* and *k* as defined in Eq. (6), can be obtained from the plot of $(\delta_{para})_{i,a}/\langle S_z \rangle_a$ versus $(\delta_{para})_{k,a}/\langle S_z \rangle_a$ within the cation series *i* . So, every deviation from linearity along the series can be attributed to a structural change affecting G_i or variations in the ligand field.

Because $<S_z>_a$ values for actinide cations are not known this study is performed only with the complexes formed with the Ln(III) cations (**Figure 3**). The plots for two pairs of protons H_3/H_5 and H_5/H_6 show linear variations excluding any drastic change of the geometric ratios R_{ik} along the Ln series. This could be explained by the division of the experimental paramagnetic shifts by $<S_z>_a$ smoothing the variation of the geometric factor ratio previously obtained in **Table 1**. One deduces from the intercepts that the hyperfine coupling constants F_i do not change along the Ln series for the protons. However Eq. (7) plotted for carbons and proton H_6 pairs exhibit two kinds of straight lines along the Ln series (**Figure S10**). The slopes for the lightest Ln (Ce to Eu) and the heaviest ones (Tb to Yb) are parallel, except for carbons C_2 and C_6 where the plots show a poor correlation for the lightest Ln(III). It can be concluded that the F_i values depend on light or heavy Ln(III) while the geometric factor G_i does not change along the Ln series.

Separation of contact and dipolar shifts, one nucleus method:

Separation methods[3f], using the chemical shifts induced by the lanthanide cations for a group of complexes are based on rearrangements of Eq. (4) in two equations:

$$\frac{(\delta_{para})_{i,a}}{<S_z>_a} = F_i + G_i A_2^0 < r^2 > \frac{c_a^D}{<S_z>_a} \quad (8)$$

$$\frac{(\delta_{para})_{i,a}}{c_a^D} = F_i \frac{<S_z>_a}{c_a^D} + G_i A_2^0 < r^2 > \quad (9)$$

Based on the following assumptions: 1- F_i and G_i are independent of the Ln(III) ion a; 2- the crystal field parameter is invariant along the series; 3- theoretical values of $<S_z>_a$ and C_a^D are known, the graphic representation of Eqs. (8) and (9) for a given nucleus i and varying the Ln center a are linear and the slopes provide the dipolar and contact terms respectively.

It has been shown that the use of Eq. (8) provides better accuracy for the determination of the crystal field parameter $A_2^0 < r^2 >$ while Eq. (9) is more appropriate to determine F_i[21]. Both equations are applied hereafter to the $[Ln(ethyl\text{-}DPA)_3]^{3-}$ series.

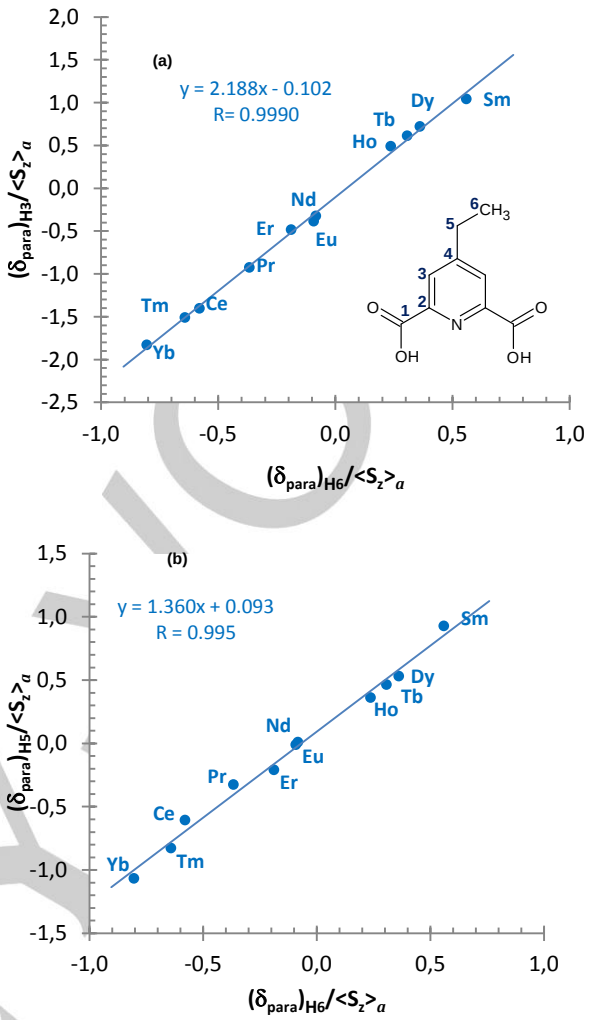

Figure 3. Plot of Eq. (7) for $[Ln(ethyl\text{-}DPA)_3]^{3-}$ in DMSO-d6 (at 298K). **(a)** H_3 *vs* H_6 and **(b)** H_5 *vs* H_6.

Determination of $A_2^0<r^2>$ parameter:

The plot of Eq. (8), presented in SI (**Figure S2**), shows an excellent linearity (R > 0.99) except for Sm(III) and Ce(III) cations particularly for proton H_5. As expected the ratio of H_3 and H_5 slopes divided by the H_6 one leads to G_{H_3}/G_{H_6} = 2.20 and G_{H_5}/G_{H_6} =1.37 which are in good agreement with the R_{ij} values of **Table 1**. This validates the hypothesis that the crystal field parameter $A_2^0 < r^2 >$ is almost invariant along the lanthanide series in the ethyl-DPA. The crystal field parameter deduced from the slope and the geometrical factor G_i defined in Eq. (5) for each proton are given in **Table 2** ; This constancy observed along the series (Ce – Yb) contrasts somewhat with some studies including macrocyclic ligands (DOTP).[14c] Indeed, the study of heavy lanthanides (Tb – Yb) revealed a $A_2^0 < r^2 >$ parameter different for each cation. However, the crystal field induced by this highly complexing ligand was found about 50 times higher than in our study. It can therefore be considered that a lower crystalline field can lead to smooth the modifications observed in the study of $[Ln(DOTP)]^{5-}$ complexes. Moreover, $A_2^0 < r^2 >$ parameters were calculated by these authors, considering that the chemical shifts of ^1H nuclei were only dipolar which is not fully established. This assumption can be at the origin of the observed variations which are not linear along the series.

The plots of Eq. (8) for ^{13}C C_1-C_6 are presented in **Figure S3**. Unlike ^1H nuclei, there is no clear linear trend for the whole series (Ce – Yb) but one finds a good linear regression for the six heaviest cations (from Tb to Yb) and a different one for three of the lightest ones (Pr, Nd and Sm), Ce and Eu being for most plots out of these lines. This can mean a change in the crystal field parameter $A_2^0\langle r^2\rangle$ or a variation of geometric term G_i between the beginning and end of series. However, the first elements are described by only three cations and changes seem to occur for Ce(III) and Eu(III) which can lead to uncertainties in determining the crystal field parameter. Therefore, the crystal field parameter was calculated only with results achieved on the heaviest cations (from Tb to Yb). The crystal field values (**Table 2**) reveal a good agreement with the ^1H NMR study that confirms the value of this parameter for the Ln(III) cations. It may be noted that the ^{13}C spectral width is greater than that of the ^1H, therefore enhancing differences that could have appeared negligible in the ^1H study.

Table 2. $A_2^0\langle r^2\rangle$ crystal field coefficient (in cm^{-1}) of $[Ln(ethyl\text{-}DPA)_3]^{3-}$ complexes deduced from the slopes **Figure S2** and **S3** and G_i for a given nucleus (4th column) and averaged for all ^1H and all ^{13}C (last column).

			$A_2^0\langle r^2\rangle$	
Ln^{3+}	^1H	H_3	51.6	52 (±1)
		H_5	52.5	
		H_6	49.0	
Tb^{3+} – Yb^{3+}	^{13}C	C_3	44.6	51 (±4)
		C_4	55.4	
		C_5	49.8	
		C_6	54.2	

Determination of F_i parameters:

$(\delta_{para})_{i,a}/C_a^D$ versus $\langle S_z\rangle_a/C_a^D$ is plotted in **Figure S4** for ^1H nuclei and in **Figure S5** for ^{13}C nuclei for the whole lanthanide series. According to Eq. (9), these plots should be linear and the slope gives the value of F_i for the nucleus of interest. The points for the ^1H in Ce(III) and Eu(III) cations lie out and were not considered to determine the F_i terms. In all cases, two straight lines are obtained, one for the 1st part (Pr – Sm) and another one for the 2nd part (Tb – Yb) of the series. Better correlations are found for ^{13}C than for ^1H data due to higher F_i parameters for carbon nuclei. F_i deduced from these plots are tabulated in **Table 3**.

The break of slope in the middle of the series is often observed and usually assigned to a change in F_i and $A_2^0\langle r^2\rangle$ parameters induced by structural changes.[2b] However we deduced from the previous section that the crystal field parameter $A_2^0\langle r^2\rangle$ may be considered invariant along the series. Moreover the crystallographic study by single-crystal XRD shows that $[Ln(ethyl\text{-}DPA)_3]^{3-}$ complexes are isostructural along the series. The small decrease observed on bonds length Ln - O and Ln - N along the series leads to a geometric parameter variation almost invisible which cannot explain this drastic change. In 2002, Ouali *et al.* have tried to explain this slope break for lanthanide complexes with dipicolinic acid by a rapid oscillation of the pyridine cycle at the NMR time scale.[5a] However, the agreement between the results obtained by MD simulations and the chemical shifts analysis do not show such flexibility of our complexes and therefore do not confirm the impact of this phenomenon.[5b, 14a, 14b] Furthermore, this break occurs always in the middle of the series (Eu – Tb).[5, 14a, 14b, 22] It can thus be considered that a change in the electronic structure could lead to a variation in the hyperfine coupling constant in the $[Ln(ethyl\text{-}DPA)_3]^{3-}$ complex.[5b]

Table 3. F_i parameters (dimensionless) obtained from the $(\delta_{para})_{i,a}/C_a^D$ versus $\langle S_z\rangle_a/C_a^D$ plots of ^1H and ^{13}C paramagnetic shift for $[Ln(ethyl\text{-}DPA)_3]^{3-}$.

		Tb – Yb	Ce – Eu
^1H	H_3	0.035	-0.016
	H_5	0.094	0.210
	H_6	0.038	0.055
^{13}C	C_1	-1.303	2.447
	C_2	-0.192	0.360
	C_3	-2.728	-4.384
	C_4	1.303	1.642
	C_5	-0.187	-0.422
	C_6	0.192	0.450

Separation of contact and dipolar shifts, three nuclei method:

In 2001, Geraldes *et al.* proposed an analysis method of paramagnetic shift independent of $\langle S_z\rangle_a$ and C_a^D theoretical values.[14a, 23] This method is particularly interesting in this case because the constancy of F_i and G_i parameters can be checked along a series of cations without a prior knowledge of theoretical $\langle S_z\rangle_a$ and C_a^D values (unknown for the actinides) and independently of the crystal field parameter $A_2^0\langle r^2\rangle$. It is based on the exploitation of experimental data obtained on three nuclei *i*, *j* and *k* of the same metallic complex by the following equations:

$$\frac{(\delta_{para})_i}{(\delta_{para})_j} = \alpha\frac{(\delta_{para})_k}{(\delta_{para})_j} + \beta \qquad (10)$$

$$\alpha = \frac{(S_{ij}-R_{ij})}{(S_{kj}-R_{kj})} \qquad \beta = \frac{(S_{kj}R_{ij}-S_{ij}R_{kj})}{(S_{kj}-R_{kj})}$$

$S_{ij} = \frac{F_i}{F_j}$ R_{ij} defined in Eq. (6).

Study of ^1H nuclei:

The plot of Eq. (10) for ^1H nuclei shows a slight difference between the light and heavy lanthanides as shown in **Figure 4**. This variation can be assigned to the F_i change along the lanthanide series like previously observed.

Regarding An(III) cations, it can be noted that a straight line (**Figure 4**) fits nicely the ^1H paramagnetic shifts. This feature indicates that a single set of parameters G_i and F_i allows to describe the properties of these cations. Since the An(ethylDPA) series is isostructural to the Ln(III) one ($R_{36} = 2.1$ and $R_{56} = 1.3$), the strong difference between these two cation series is due to F_i values: they are different from the Ln(III) one and are constant along the series (at least from Pu to Cf). Unfortunately this method does not provide quantitative values of F_i.

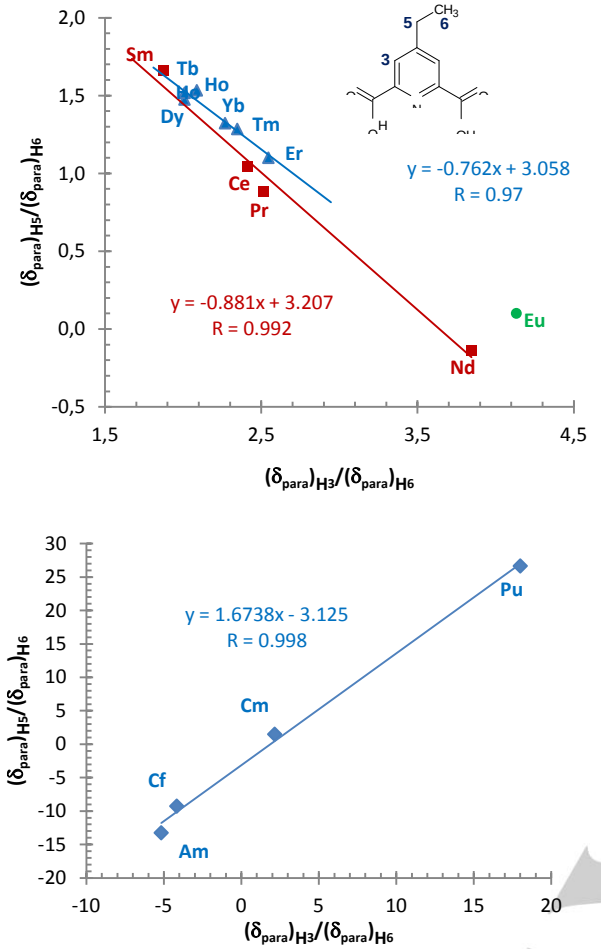

Figure 4. Plots of $(\delta_{para})_{H5}$ / $(\delta_{para})_{H6}$ vs. $(\delta_{para})_{H3}$ / $(\delta_{para})_{H6}$ for $[Ln(ethyl\text{-}DPA)_3]^{3-}$ (up) and $[An(ethyl\text{-}DPA)_3]^{3-}$ (down) in DMSO (at 298K). Eu(III) is excluded from the linear regression calculation of light Ln(III).

Study of ^{13}C nuclei:

The study of ^{13}C chemical shifts by this method reveals a much more marked difference between heavy and light Ln(III) cations (**Figure S6**). The values of α and β terms determined by this method and summarized in **Table 4** are in quite good agreement with the values calculated from Eq. (10) with F_i and G_i parameters terms determined previously (See **Table S5** for G_i values). Main differences occur for α values with the lightest Ln and β values of C_1 nucleus. The first remark could be related by a defect in Bleaney's approach of the dipolar contribution in the lightest Ln(III) series as we mentioned previously while the second could be due to a structural change close to the metal center since we already have taken into account the F_i change.

Regarding the ^{13}C paramagnetic shifts of An(III) complexe, only three cations (Pu, Am and Cf) have been studied because the Cm(III) induces animportant line broadening preventing analysis. It can be noted that straight lines describe pretty well the chemical shift evolutions although a slight deviation appears on C_3 and C_4 nuclei (**Figure S6**).

To support the structural change assumption, a sampling of the structure of $[Dy(ethyl\text{-}DPA)_3]^{3-}$ complex was performed by MD calculations. The distance Dy(III)-nitrogen of the pyridine ring and the angle formed between this direction and the axis of highest symmetry Z were kept constant all along the calculation (Z axis is taken perpendicularly to the plan formed by the three nitrogens of the complex). The structures having the best agreement with the geometric terms ratios show a slight variation in the position of the pyridine ring compared to the central cation and the main axis of magnetic susceptibility (Z) as shown in **Figure 5**. This configuration leads to oxygen atoms away from each other in the tricapped trigonal prism which minimizes the interatomic repulsion. This could explain that atoms close to the paramagnetic center, especially the carbon atom of the carbonyl group (C_1) for which the geometric term (G_i) is strongly influenced by the angle θ_i may be sensitive to small radii contractions along a series.

Table 4. α and β parameters obtained from the plots $(\delta_{para})_{Ci}$ / $(\delta_{para})_{C6}$ *vs.* $(\delta_{para})_{C5}$ / $(\delta_{para})_{C6}$ (**Figure S6**) of ^{13}C paramagnetic shift for $[Ln(ethyl\text{-}DPA)_3]^{3-}$. [a] α and β calculations from Eq. (10) using F_i from **Table 3** and geometrical factors from structural data with *i* the corresponding ^{13}C, *j*=C_6 and *k*=C_5.

		α	α [a]	β	β [a]
Tb – Yb	C_1	3.29	2.92	-0.33	-3.94
	C_2	4.20	4.13	4.42	3.025
	C_3	7.47	7.56	-6.65	-6.85
	C_4	-1.59	-1.63	5.08	5.20
Ce – Eu	C_1	0.68	-2.12	7.15	3.45
	C_2	2.73	3.31	3.60	3.90
	C_3	4.58	5.74	-5.28	-4.36
	C_4	0.57	-0.32	4.23	3.35

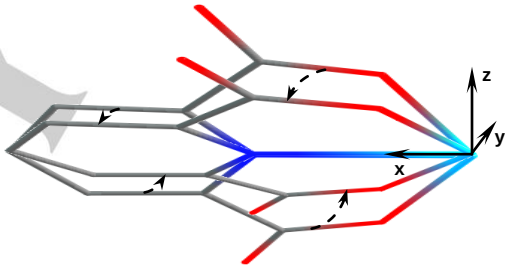

Figure 5. Movement of the pyridine ring along the main axis of magnetic susceptibility Z.

From room temperature experiments and within Bleaney's theory we conclude that the G_i parameters are almost constant along the series while F_i depends on the Ln(III) since two sets of values are determined, the crystal field parameter is constant along the Ln series (about 51 cm^{-1}) and the contact term is the main contribution in the An paramagnetic shifts even far from the metallic center.

2.3. Temperature variation of ^1H and ^{13}C chemical shifts

Temperature effects on the induced paramagnetic shifts provide further information on Bleaney's parameters, $\langle Sz \rangle_a$ and C_a^D since they are temperature dependent.

Ln(III):

^1H and ^{13}C paramagnetic shifts of $[Ln(ethyl\text{-}DPA)_3]^{3-}$ complexes were recorded over temperature range 20 - 70°C every 5°C. $[La(ethyl\text{-}DPA)_3]^{3-}$ complex was used as diamagnetic reference. The separation of contact and dipolar contributions may be obtained assuming a 1/T dependence for the former and a $1/T^2$ dependence for the latter as proposed by Bleaney.[6a] The experimental results are shown as $\delta_{para}.T = \frac{\rho}{T} + \varepsilon = f(1/T)$ on **Figure 6** for Yb(III) complex (see **Figure S7** for other

lanthanides); within the previous assumptions, the slope ρ and the intercept ε provide the dipolar and contact contributions respectively (reported **Tables S6** and **S7**). In all cases a nice linear correlation is observed. Except for C_5 of Ce(III) complex all ^{1}H contact contributions are much smaller (in absolute values) than those of the ^{13}C; As expected, the farthest protons from the paramagnetic center (H_5 and H_6) present the smallest contact contributions except for the Sm(III) case for which H_3 contact term is surprisingly smaller. Actually all contact Sm(III) values significantly deviate from the other Ln(III) cations.

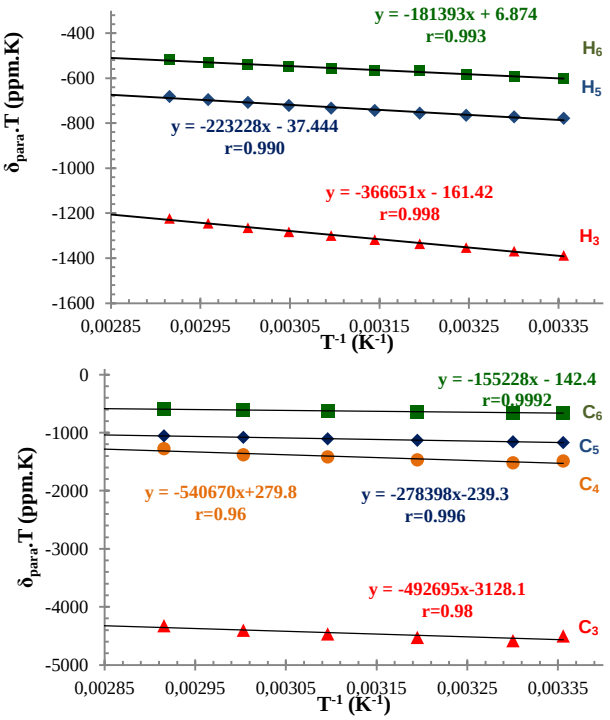

Figure 6. Product of the temperature T with ^{1}H (top) and ^{13}C (bottom) paramagnetic shifts *versus* 1/T for [Yb(ethyl-DPA)$_3$]$^{3-}$ complexes.

For [Yb(ethyl-DPA)$_3$]$^{3-}$ complex, extrapolations to T^{-1}=0 of all analyzed protons lead to the smallest ε values (close to 0) as observed in previous studies on [Ln(DPA)$_3$]$^{3-}$ complexes in aqueous solution.[3c] This suggests that the paramagnetic shift of protons is mainly dipolar. Regarding the ^{13}C, contact contributions of C_1 to C_3 cannot be neglected since εT at room temp and ρ get closer. Regardless the Yb(III) case, it comes from Eq. (4) that ε should be equal to $298\langle S_z\rangle_a F_i$. A plot of ε values *vs* $\langle S_z\rangle_a$ tabulated by Pinkerton *et al.*[7] at 298K for all Ln(III) and nuclei confirms the good correlation except for C_6, H_5 and H_6. These nuclei far from the paramagnetic center experience a low contact interaction that could account for this low correlation coefficient. Surprisingly the C_1 nucleus supposed to have significant contact contribution exhibits a poor correlation with $\langle S_z\rangle_a$. **Tables S6** and **S7** summarize the F_i values calculated by this way (calculated as $\varepsilon/298\langle S_z\rangle$). For most of them they are of the same order of magnitude as those of **Table 3** but vary in the series, both in value and sign for values close to zero. The discrepancy between both ways of calculation is about 150%.

According to Eq. (4) and assuming that the crystal field parameter is constant in the series, the ratio of the slopes ρ_{ia}/ρ_{ib} for a given nucleus *i* should be equal to the ratio of Bleaney's parameters[6a] C_a^D (normalized to C_{Dy}^D =-100) but this is not confirmed by results given in **Table 5** despite values are of the same magnitude order for the heaviest Ln(III).

These observations arising from both contributions (contact and dipolar) seem to reveal that the paramagnetic shifts, induced by the Ln(III) cations, are not accurately described by considering a variation of the dipolar and contact contributions with T^{-2} and T^{-1} respectively. To explain these differences, it can be considered that a part of this contribution can vary with T^{-n} (n > 2). In fact, the pseudocontact term was treated by Bleaney[6] as a series of T^{-n} terms assuming that the first nonzero term in T^{-2} is predominant. Nevertheless, significant deviations between theory and experimental data have appeared. In 1970, Kurland and McGarvey showed more complex behavior deriving the general formula of the dipolar contribution in terms of magnetic susceptibility.[24] Later, McGarvey performed a theoretical study to determine the amplitude of T^{-n} terms for several lanthanide ions[25]. It has been established that although the temperature dependence is not exactly T^{-2}, an accuracy of about 10 - 20% can be obtained at room temperature.

Table 5. Slope ρ_{ia} of the $\delta_{para}.T = f(1/T)$ plot for H_6; ratios normalized at -100 for Dy(III) and C_a^D calculated by Bleaney[6a].

M(ethyl-DPA)$_3^{3-}$	ρ_{6a}	$-100\rho_{ia}/\rho_{iDy}$	C_a^D
Ce	27551	-2.8	-6.3
Pr	77706	-7.9	-11
Nd	-29691	3.0	-4.2
Sm	-19769	2.0	-0.7
Eu	-99737	10.1	4
Tb	1129070	-114.5	-86
Dy	986106	-100.0	-100
Ho	595106	-60.3	-39
Er	-274775	27.9	33
Tm	-463358	46.9	53
Yb	-181393	18.4	22

This discrepancy may be overcome by adding a T^{-3} term to the dipolar term. LaMar *et al.*[26] showed a detailed expression of the contact term by computing the components of the magnetic susceptibility tensor through the Van Vleck equation.[26] Substituting these terms in the contact contribution expression leads to the appearance of two terms varying as T^{-1} and T^{-2} (S'_a and S''_a respectively in Eq. (11)) although the latter is not predominant. It can be considered that this term may be involved in our lanthanide complexes.

In order to check the applicability of these two assumptions, an adjustment of the ^{1}H and ^{13}C experimental results was performed according to the following equation:

$$\left(\delta_{para}\right)_{i,a} = \frac{F_i}{T}\left[1+\frac{\tau_1}{T}\right]S'_a + \frac{G_i}{T^2}A_0^2 < r^2 > \left[1+\frac{\tau_2}{T}\right]C'_a \qquad (11)$$

This supposes that $\langle S_z\rangle_a = \frac{S'_a}{T} + \frac{S''_a}{T^2}$ with the ratio $\tau_1 = \frac{S''_a}{S'_a} = cste$ and $C_a^D = \frac{C'_a}{T^2} + \frac{C''_a}{T^3}$ with the ratio $\tau_2 = \frac{C''_a}{C'_a} = cste$. S'_a, τ_1, C'_a and τ_2 are considered independent on nucleus *i* ; their values were optimized for each Ln(III) with an Excel solver using the experimental data for three ^{1}H (H_3, H_5 and H_6) and six ^{13}C (C_1, C_2, C_3, C_4, C_5 and C_6) nuclei and the geometric parameters G_i defined by MD calculations and are summarized in **Tables S9** and **S6**. C_{Dy}^D and $\langle S_z\rangle_{Gd}$ are respectively set to -100 and 31.5 respectively. The results of the adjustment procedure (Excel solver) are shown in **Table 6**. All experimental values and

calculated parameters are detailed in **Tables S8**, **S9** and drawn in **Figure S11**.

Table 6. Parameters of ^{1}H and ^{13}C paramagnetic shifts adjustment for $[Ln(ethyl\text{-}DPA)_3]^{3-}$. τ_1 and τ_2 are defined in Eq. (11). They represent temperature deviations of the contact and dipolar contributions respectively in Bleaney's equation at T = 300K.

	Contact $\frac{\tau_1}{T}$	Dipolar $\frac{\tau_2}{T}$	Deviation calc./exp.	
			^{1}H	^{13}C
Ce	0.45	0.68	3.2%	5.0%
Pr	0.11	0.26	1.8%	13%
Nd	0.87	0.11	17%	3.1%
Sm	0.89	0.56	5.1%	22%
Eu	0.33	0.14	21%	3.0%
Tb	-0.03	0.47	0.4%	2.1%
Dy	0	0.20	0.5%	5.8%
Ho	-0.04	0.51	1.1%	3.2%
Er	-0.01	-0.13	0.6%	1.1%
Tm	0.09	0.00	0.6%	1.2%
Yb	0	-0.18	0.5%	1.0%

The results of this adjustment procedure clearly show that τ_1 (T^{-2} contact term) is negligible for Tb(III) to Yb(III) cations while T^{-2} contact and T^{-3} dipolar terms are both required for all the lightest Ln(III). For the heaviest Ln(III), it may be noted that the influence of τ_2 (T^{-3} dipolar term) is different for the latter since there is no contribution for Tm(III) and negative ones for Er(III) and Yb(III). The greater T^{-3} contributions belong to the formers with up to 32% for Tb(III) and Ho(III). This is in agreement with recent results of Hiller *et al.* mentioning that the magnetic anisotropy χ_{as} (which is another description of the dipolar contribution, see Quantum chemistry calculations section) of Ho(III) complexes deviates from a T^{-2} behavior.[27]. The greatest τ_1 and τ_2 values are observed for the lightest cations (from Ce to Eu) with a significant contact T^{-2} term up to 47% for Sm(III) and Nd(III) and a large T^{-3} dipolar contribution up to 40% for Ce(III). Large deviation between experimental and fitted data (22% for ^{13}C and 21% for ^{1}H) are also observed for the light Ln. This is explained by the smallness of paramagnetic chemical shift variations collected in Sm(III) and Nd(III) cases.

The fit reveals almost constant F_i parameters within 51 and 26% deviation (average of the relative differences between F_i and $\langle F_i \rangle$ along the Ln(III) series) for light and heavy Ln respectively. A broader F_i distribution (variation over 100%) is however observed for H_3, C_1 and C_2 nuclei whatever the Ln(III) set. Except for these cases, F_i values along the Ln(III) series are found similar with those collected **Table 3** and this confirms that light and heavy Ln(III) have different set of F_i values. The use of F_i values with geometric parameters G_i leads to α and β values which are in good agreement (average of 20% excluding data from C_1) with the slopes (α) and intercepts (β) deduced from δ_{para} ratios Eq. (10).

Regarding the crystal field parameter $A_2^0\langle r^2 \rangle$, an average of 51.1 and 52.5 cm^{-1} within a 2% deviation is obtained for light and heavy Ln(III) respectively which is consistent with the results of **Table 2**. $\langle S_z \rangle_a$ and C_a^D parameters issued from this fit are the same than those of Pinkerton[7] and Bleaney[6a] at 300K except for Sm(III) for which $\langle S_z \rangle_a$ is found to be 0.26, 19% larger than the Pinkerton's values (See **Table S9**).

An(III):

^{1}H and ^{13}C paramagnetic shifts of $[An(ethyl\text{-}DPA)_3]^{3-}$ complexes were studied in the range 20 - 80°C using $[La(ethyl\text{-}DPA)_3]^{3-}$ as diamagnetic reference. As for Ln(III) complexes, a linear variation of paramagnetic shifts versus 1/T was observed for each nucleus of the ligand (**Figure 7** for the Cf(III) example and **Figure S8** for all other An(III) cations).

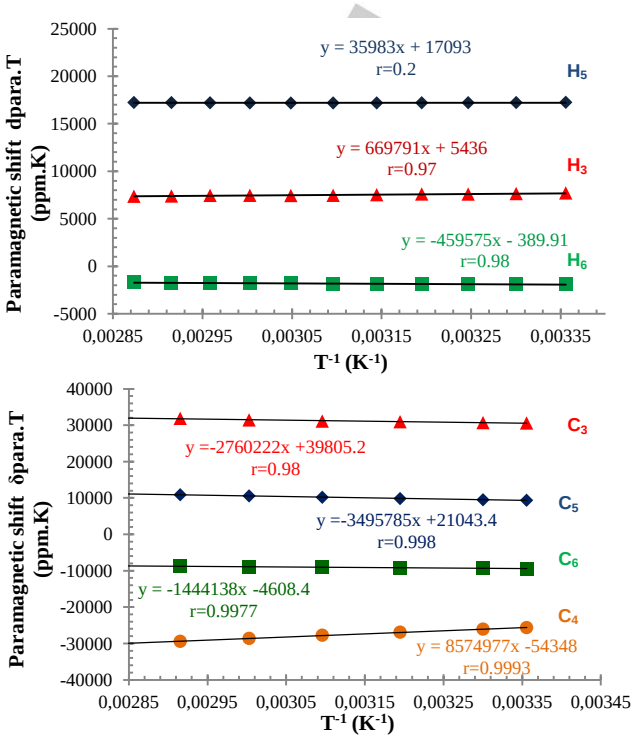

Figure 7. Product of the temperature by the ^{1}H and ^{13}C paramagnetic shift versus 1/T for the $[Cf(ethyl\text{-}DPA)_3]^{3-}$ complex.

It is surprising to observe that the intercepts for protons (H_3, H_5, H_6) of the $[Pu(ethyl\text{-}DPA)_3]^{3-}$ complex exhibit values close to 0 (-22; -27 and 1 for H_3, H_5 and H_6 respectively). This suggests a vanishing contact term which is clearly inconsistent with ^{1}H paramagnetic shift ratios of **Table 1** suggesting a large contact contribution. Conversely, the nonzero intercept (116 and 335 respectively) for H_3 and H_5 protons of Am(III) are more consistent with results of **Table 1** showing a contact contribution. Regarding Cm(III), a very high intercept for all protons of ethyl-DPA ligand, including the CH_3 group (H_6) which displays usually only a dipolar contribution (4555; 5306 and 3240 for H_3; H_5 and H_6 respectively) in contradiction with **Table 1** suggesting (maybe fortuitously) a predominant dipolar contribution for all protons. Finally, the analysis of the ^{1}H signals of $[Cf(ethyl\text{-}DPA)_3]^{3-}$ complex reveals a behavior similar to that of Am(III) with a nonzero intercept for H_2 and H_5 protons but close to 0 for the CH_3 group. To overcome these discrepancies, T^{-2} and T^{-3} contact and dipolar contributions respectively have to be taken into account, like for Ln(III) complexes.

A fit of the An(III) experimental data was performed using Eq. (11) with the same procedure as for the Ln(III) series. Results are collected in **Table 8**. A significant T^{-3} dipolar term is observed for all studied An(III) except for Cm(III) (about 38 to 86% of the total dipolar contribution). Unlike the Ln(III) series all the S''_a contributions are negative. The contact T^{-2} term is important for Am(III) and more significantly for Pu(III) since they account for about 29% and up to 46% of the total contact contribution respectively. On the contrary Cm(III) and Cf(III) present negligible T^{-2} contact contributions. The absence of

extra T^{-2} contact and T^{-3} dipolar terms for Cm(III) coincides with the purely T^{-2} dipolar contribution found in **Table 1**. However we have to keep in mind that only 3 nuclei (only protons, no carbon at all) have been analyzed instead of 9 unlike the other An(III) cations. A low number of experimental data leads to a fit with a lower deviation.

Similarly to the Ln(III) series, deviations from T^{-1} contact (S''_a) and T^{-2} dipolar (C''_a) are observed for the lighter An(III) (with Pu(III) and Am(III)) while there is only T^{-2} dipolar deviation for the heavier An(III) (Cf(III)).

Table 8. Parameters of ^{1}H and ^{13}C paramagnetic shifts adjustment for $[An(ethyl\text{-}DPA)_3]^{3-}$. τ_1 and τ_2 are defined Eq. (11). They represent temperature deviations of the contact and dipolar contributions respectively in Bleaney's equation at T=300K. #geometrical parameters used from ref [15] .

An(III) (isoelectronic 4*f*)	*Contact* $\frac{\tau_1}{T}$	Dipolar $\frac{\tau_2}{T}$	Deviation calc./exp.	
			^{1}H	^{13}C
Pu (Sm)	0.85	-0.86	3.5%	2.7%
Am (Eu)	-0.31	-0.53	3.5%	2.7%
Am#	-0.40	-0.58	4.0%	2.1%
Cm# (Gd)	0.01	0	0.54%	/
Cf# (Dy)	-0.06	-0.38	2.04%	3.0%

The use of two different crystallographic sources (our XRD results and Cary *et al.* study) lead to slight differences in calculated geometric parameters of the $Am(ethyl\text{-}DPA)_3^{3-}$ complex especially for C_1, C_3 and H_3 nuclei (25, 3 and 7% respectively; see **Table S5**). Owing to these geometrical variations and their use in Eq. (11), the optimization procedure led to deviations of 13 and 5% for τ_1 and τ_2 respectively (**Table 8**) but does not affect the $\langle S_z \rangle_a$ and C_a^D values (**Table 9**). It is noteworthy that $\langle S_z \rangle_a$ and C_a^D deduced at 300K are not sensitively different than those of the isoelectronic Ln(III) configurations (**Table 9**; for more details see **Table S11**). Surprisingly the An(III) crystal field parameter $A_0^2 < r^2 >$ obtained from these adjustments is found close to the Ln(III) cation value: $A_0^2 < r^2 >$=52±1 cm^{-1}.

Table 9. $\langle S_a \rangle$ and C_a^D values determined for An(III) cations at T=300K and compared to literature [6b, 7] for a same 4*f* electronic configuration. #geometrical parameters used from ref [15] .

$An(ethyl\text{-}DPA)_3^{3-}$	$\langle S_z \rangle_a$	$\langle S_z \rangle_a$ [7]	C_a^D	C_a^D [6b]
Pu	0.45	0.22 (Sm)	-0.6	-0.7 (Sm)
Am	10.93	7.57 (Eu)	3.8	4 (Eu)
Am#	10.76		3.8	
Cm#	31.52	31.5 (Gd)	0	0 (Gd)
Cf#	28.56	28.57 (Dy)	-99.0	-100 (Dy)

Regarding F_i values, only one data set has been considered to study the An(III) conversely to the Ln(III) series. Maybe as a result it has been difficult to find constant F_i values since deviations are all greater than 100% (average of the relative differences between F_i and $\langle F_i \rangle$ along the An(III) series)). The maximum deviation is reached for H_6 with 420% (**Table S11**). Calculations of α and β parameters from these F_i values and geometric parameters G_i lead to values that are not in good agreement (160% for ^{13}C and 55% for ^{1}H in average) with the slopes (α) and intercepts (β) deduced from δ_{para} ratios Eq. (10). Based on the Eq (10) assumptions, this feature emphasizes the non constancy of the F_i values along the An(III) series and consequently, the difficulty to separate the paramagnetic contributions in Bleaney's equation for the An(III). When looking at paramagnetic shifts *vs* 1/T plots (**Figures S12**) it comes out that to go further more data are required especially from temperature experiments. An organic diluent in liquid state over a larger temperature range would be required to get an optimization processing more accurate.

2.4. Quantum chemistry calculations

Since $\langle S_z \rangle_a$ and C_a^D values are not available for the actinide series, they were determined by quantum chemistry calculations first within the Ln(III) series in order to check and validate the methods. First principle calculations with SO-CASSCF and SO-CASPT2 have been performed in the $Ln/An(DPA)_3$ series using the crystallographic data except for U(III) and Np(III) complexes were the geometries were optimized by DFT calculations. *z* axis is taken along the pseudo C_3 axis perpendicular to the plan formed by the three nitrogens. The average of the electron spin magnetization $\langle S \rangle_a$ has been evaluated along three directions and averaged to $\langle S_m \rangle_a$ (see **Tables 10** and **11** for Ln(III) and An(III) respectively). C_a^D describes the anisotropy of the magnetic susceptibility $C_a^D = \chi_{//} - \chi_{\perp}$ and has been deduced from SO-CASPT2 magnetic susceptibility calculations along x, y, z axes according to $C_a^D = \chi_z - (\chi_x + \chi_y)/2$ [28] and are collected in **Tables 12** and **13** for Ln(III) and An(III) respectively.

Electron spin magnetization <S>*a* calculations

Ln(III):

As expected for a spin contribution, the $\langle S \rangle_a$ anisotropy is relatively small, comprised between 19% for Ce(III) and 34% for Sm(III). Consequently we will discuss hereafter the average of calculated $\langle S \rangle_a$ in all directions ($\langle S_m \rangle_a$) as representative of experimental $\langle S_z \rangle_a$ values.

Table 10. SO-CASSCF $\langle S \rangle_a$ values for $[Ln(DPA)_3]^{3-}$ complexes in three directions of space, averaged and from literature. The last column gives the relative difference between $\langle S_m \rangle_a$ and $\langle S_z \rangle_a$ from Golding *et al.*[29] and Pinkerton *et al.* [7] at 300K. All values are scaled to 31.50 for Gd(III).

	$\langle S_x \rangle_a$	$\langle S_y \rangle_a$	$\langle S_z \rangle_a$	$\langle S_m \rangle_a$	$\langle S_z \rangle_a$ [29]	$\langle S_z \rangle_a$ [7]	Diff
Ce (f^1)	-0.78	-0.65	-1.08	-0.84	-0.98	-0.97	15.5%
Pr (f^2)	-2.83	-2.59	-3.00	-2.8	-2.97	-2.96	5.7%
Nd (f^3)	-4.12	-3.97	-4.45	-4.18	-4.49	-4.45	6.5%
Sm (f^5)	0.39	0.22	0.62	0.41	-0.06	0.22	46.3%
Eu (f^6)	11.12	11.59	10.11	10.94	10.7	7.57	30.8%
Gd (f^7)	31.50	31.50	31.50	31.50	31.50	31.50	0.0%
Tb (f^8)	30.38	27.86	37.69	31.98	31.82	31.85	0.4%
Dy (f^9)	27.93	26.24	31.65	28.61	28.55	28.57	0.1%
Ho (f^{10})	22.36	21.80	23.53	22.56	22.63	22.64	0.4%
Er (f^{11})	15.56	15.89	14.68	15.37	15.38	15.38	0.1%
Tm (f^{12})	8.49	9.51	6.54	8.21	8.21	8.21	0.0%
Yb (f^{13})	2.66	2.89	2.15	2.57	2.59	2.59	0.8%

The calculated $\langle S_m \rangle_a$ values are roughly in good agreement with the published ones. The agreement is better for the 2nd part of the series; the ground term of the free ion corresponds to a large *J* value, the *J-1* excited state is relatively high in energy due to Landé rule. The theoretical value $\langle S_z \rangle_a$ calculated by Pinkerton[7] within the ground *J* term manifold is suitable. For the 1st part of the series, the discrepancy is larger since the low lying *J+1* manifold plays a key role.

The values determined by Pinkerton *et al.* given in **Table 10** were evaluated according to Golding's approach[29] (taking into account bonding effects, spin-orbit coupling and mixing of excited states into the ground state) for the whole series but using relativistic Hartree-Fock method and reconsidering the spin-orbit coupling which is a sensitive feature particularly for light ions. However for Sm(III) and Eu(III), they found reasonable estimation of $\langle S \rangle_a$ values in agreement with their ^{1}H and ^{31}P experiments by making adjustment or using particular value of spin-orbit coupling constant ζ or Landé factor g_J. Conversely to Pinkerton's approach, our *ab initio* $\langle S_m \rangle_a$ approach does neither consider any experimental data along the Ln(III) series nor make any assumption about $\langle S_m \rangle_a$ dependence with temperature. In such frame of mind, first of all at 300K, it is noteworthy to observe that for Sm(III), our calculated value of $\langle S_m \rangle_a$ is close to the one proposed by Pinkerton[7] while for Eu(III), the value is close to the one proposed by Golding[29]. The comparison of our experimental $\langle S_z \rangle_a$ and calculated $\langle S_m \rangle_a$ values exhibit a good agreement with the heavy Ln(III) but some deviations are observed with Ce(III) (11%) and especially with Sm(III) and Eu(III) (56 and 44% respectively).

The behavior of $\langle S_m \rangle_a$ with temperature in the 250-350 K range depends strongly on the Ln(III) ion (see **Figures S13** and values in **Table S12**). They were fitted using two model functions. First, a function with T^{-1} and T^{-2} terms as described in Eq. (11) ($T\langle S_z \rangle_a = f(T^{-1})$ plots) and Pinkerton's *et al.* approximation ($\langle S_z \rangle_a = a+bT$)[7]. Without surprise this last assumption leads to the poorest correlation coefficients. τ_1/T (T=300K) values deduced from the first function are found negligible (<<1) for Gd(III) to Yb(III) as observed experimentally expressing thereby the lack of T^{-2} term in the contact contribution as predicted in Bleaney's theory. However for Ce(III), Pr(III) and Nd(III) τ_1/T values are also found negligible which contrasts to experimental results. Interestingly, the calculated values of τ_1/T (T=300K) for Sm(III) and Eu(III) are -0.80 and -0.21 respectively which are close in absolute values to the experimental ones (0.89 and 0.33 in **Table 6**).

An(III):

$\langle S \rangle_a$ values at 300 K for the An(III) series (U(III) to Cf(III)) calculated with SO-CASPT2 are summarized in **Table 11**. They are normalized to $\langle S_z \rangle_a$=31.5 for Gd(III). U(III) and Np(III) complexes have been added for the sake of completeness even if DPA has not been investigated experimentally ; indeed the oxidation state III of these actinides is difficult to stabilize in solution with a DPA ligand. At 300 K $\langle S_m \rangle_a$ values are somewhat different from the Ln(III) counterparts mainly for the lighter An(III) cations (comparison of $\langle S_m \rangle_a$ values **Tables 10** and **11**). The anisotropy of $\langle S \rangle_a$ calculated as $\langle S_z \rangle - (\langle S_x \rangle + \langle S_y \rangle)/2$ is larger than for the isoelectronic Ln(III).

For Pu(III), $\langle S_m \rangle_a$ is quite far from its lanthanide analog Sm(III) (0.41 **Table 10**) and the model value ($\langle S_z \rangle_a$ = 0.45 in **Table 9**). We have recently shown[30] that the magnetic susceptibility of Pu(III), both experimental and calculated, is larger than the one expected within the LS scheme, mostly due to a Zeeman interaction with the first excited state $^6H_{7/2}$.

Table 11. SO-CASPT2 $\langle S_u \rangle_a$ values for $[An(DPA)_3]^{3-}$ complexes at 300 K scaled to the Gd(III) value (31.5).

		$\langle S_x \rangle_a$	$\langle S_y \rangle_a$	$\langle S_z \rangle_a$	$\langle S_m \rangle_a$
U	($5f^3$)	-3.56	-3.02	-2.18	**-2.92**
Np	($5f^4$)	-2.01	-2.79	-4.18	**-2.99**
Pu	($5f^5$)	-0.54	-0.24	-1.19	**-0.66**
Am	($5f^6$)	3.26	3.96	3.05	**3.42**
Cm	($5f^7$)	29.5	29.5	31.5	**30.2**
Cf	($5f^8$)	26.1	30.1	21.0	**25.7**

Eu(III) and Am(III) have a non-magnetic ground state. As shown by Golding, $\langle S_m \rangle_a$ is determined in Eu(III) by the population of the first excited $^7F_1$ term which lies 200 cm^{-1} above the ground state, according to our calculations. Since the spin-orbit coupling is larger in Am(III), this state lies at 1100 cm^{-1} and is not populated at room temperature and the magnetization arises only from Zeeman interaction with the ground state. It is why $\langle S_m \rangle_a$ is considerably smaller in Am(III) than in Eu(III).

The Cm(III complex is expected to have a smaller $\langle S_m \rangle_a$ value than Gd(III): The zero-field splitting of the $^8S_0$ term due to spin-orbit coupling with excited states is negligible for Gd(III) (less than 1 cm^{-1}) while 80 cm^{-1} with Cm(III). Consequently, this decreases slightly the magnetization.

$\langle S \rangle_a$ in Cf(III) is anisotropic and the average values is smaller to its lanthanide analog Dy(III) ; in this case zero-field splitting of the ground term $^6H_{15/2}$ is due to the interaction with the ligands and is expected to be larger in actinides than in lanthanides. In Dy(III), this splitting is of 260 cm^{-1} and all the states are thermally populated while it is more than 1600 cm^{-1} in Cf(III) leading to a decrease of the magnetization since not all the states are populated at room temperature.

The temperature dependence of $\langle S_m \rangle_a$ is represented and fitted in the 250 – 350 K range with the same models as for Ln(III) (**Table S13** and **Figures S14**). The best correlations are obtained with a $T\langle S_z \rangle_a = f(T^{-1})$ behavior except for Pu(III). Calculated τ_1/T (T=300K) are found negligible for Cm(III) and Cf(III) as observed experimentally. For both cations the temperature dependence of the contact contribution is consequently in agreement with Bleaney's theory. Conversely

U(III), Np(III) and Am(III) require a T^{-2} term since τ_1/T values are -0.14, -0.14 and -0.48 respectively. Regarding Am(III) it is interesting to note that this τ_1/T value is similar to the experimental one (**Table 8**). However the $\langle S_m \rangle_a$ temperature dependence of Pu(III) which is closer to a linear *f(T)* than a *f(T^{-1})* law emphasizes that Bleaney's approach is not adapted to describe properly An(III).

Dipolar coupling C_a^D calculations

Ln(III):

C_a^D values calculated with SO-CASPT2 at 300 K are given in **Table 12** and compared to Bleaney's ones and those deduced previously from experimental data. While all are of the same order of magnitude significant disparities (from 40 to 100%) are observed for Tm(III), Ce(III), Pr(III) and Tb(III) between the calculated and the other ones. Discrepancies between magnetic susceptibility anisotropy from experiments and Bleaney's theory have already been mentioned and assigned to crystal field effects: changes within the series and field splitting of Ln(III) ground state larger than *kT* (≈200 cm^{-1}) [31]. In our case it would be clearly the first assumption since the crystal field is found constant and lower than *kT* ($A_2^0\langle r^2\rangle$=52 cm^{-1}) (**Table 2**). As depicted recently by Mason *et al*[32], crystal field changes can be rather related to differences in the orientation than the degree of anisotropy of the magnetic susceptibility tensor[32]. The use of a ligand[33] leading to a tricapped trigonal prismatic more axially dissymmetric than our DPA ligand, allowed Vonci *et al.* to show that a few degree changes in the polar angles of the O donor due to ionic radii variations or solvent effects lead to minimal variations of the coordination geometry but different orientation of the major component of the magnetic susceptibility tensor. None of these features are taken into account neither in Bleaney's approach nor in our calculations since we used coordinates from crystallographic data (although validated by EXAFS results) along the series for our *ab-initio* calculations.

Table 12. SO-CASPT2 magnetic susceptibilities χ (in 10^{-8} mol.m^{-3}) along x,y,z axis at 300K and values of C_a^D, *ab-initio*, experimental (Table S9) and calculated by Bleaney *et al.*[6b] for $[Ln(DPA)_3]^{3-}$ complexes. C_a^D are normalized at -100 for the Dy(III). The last column gives the relative difference between calculated and Bleaney's C_a^D values.

	χ_x	χ_y	χ_z	C_a^D *calc*	C_a^D *exp*	C_a^D [6b]	Diff
Ce	2.64	2.31	3.46	-10.73	-6.5	-6.3	70%
Pr	6.20	5.81	6.70	-2.29	-11	-11	79%
Nd	6.32	6.13	6.73	-4.94	-4.0	-4.2	18%
Sm	1.51	1.43	1.64	-0.91	-0.7	-0.7	30%
Eu	6.91	7.08	6.60	3.05	4.0	4.0	24%
Gd	32.9	32.9	32.8	5.27	-	0	-
Tb	46.7	42.7	58.7	-172.7	-86.4	-86	101%
Dy	57.5	53.9	65.6	-100	-100.0	-100	0%
Ho	57.6	56.0	60.8	-36.0	-38.4	-39	8%
Er	48.1	49.1	45.3	37.8	32.7	33	15%
Tm	30.6	34.3	23.4	75.9	52.5	53	43%
Yb	11.0	11.9	8.83	26.3	21.1	22	20%

C_a^D temperature dependence from 250 to 350 K reveals two different behaviors along the Ln(III) series: One in agreement with a TC_a^D=*f(T^{-1})* law for the lightest Ln(III) (from Ce(III) to Gd(III) excluding Pr(III) for which a better correlation coefficient is obtained with a $T^2C_a^D$ = *f(T^{-1})* law) and a $T^2C_a^D$=*f(T^{-1})* law for the heaviest cations. Calculations clearly show that the second half of the An(III) series requires an additional T^{-3} term for the dipolar contribution as suggested in Eq. (11) with the experimental values. However τ_2/T values at T = 300 K deduced from the slope and intercept ratios (**Figures S15**) differs from the experimental one (see **Table 6)**: 0.22, -0.27, -0.33, -0.35, -0.20 and -0.30 from Tb(III) to Yb(III) respectively.

An(III):

Calculated C_a^D values for An(III) (**Table 13**) are quite different from the corresponding Ln(III) ones as mentioned previously but also from the experimental An(III) results.

Table 13. SO-CASPT2 magnetic susceptibilities χ (in 10^{-8} mol.m^{-3}) along x,y,z axis at 300K and values of C_a^D, *ab-initio*, experimental (**Table S11**) and calculated by Bleaney *et al.*[6b] (for 4*f* isoelectronic configuration) for $[An(DPA)_3]^{3-}$ complexes at 300K. C_a^D are normalized at -100 for Dy(III) and χ are in 10^{-8} mol.m^3 unit.

	χ_x	χ_y	χ_z	C_a^D *calc*	C_a^D *exp*	C_a^D [6a]
U	4.08	3.71	3.22	**26.8**	-	-4.2 (Nd)
Np	1.81	2.12	3.40	**-41.4**	-	2 (Pm)
Pu	0.73	0.76	0.69	**0.24**	-0.6	-0.7 (Sm)
Am	1.75	2.12	1.66	**-5.94**	3.8	4.0 (Eu)
Cm	31.1	31.2	33.3	**-49.2**	0	0 (Gd)
Cf	56.3	65.1	45.2	**50.3**	-99	-100 (Dy)

However calculations are in agreement with the experimental results in the sense that they predict an increasing anisotropy from Pu(III) to Cf(III) except for the Cm(III) appearing as the most isotropic cation according to the experimental results.

Except for χ_z value of Cm(III) and χ_y value of Cf(III) calculated An(III) magnetic susceptibilities are smaller than the corresponding Ln(III) values. This was experimentally observed by Cary *et al.*[15] comparing magnetic susceptibilities of $Cf(DPA)_3.H_2O$ and $Dy(DPA)_3.H_2O$ complexes and explained by a large ground state $^6H_{15/2}$ splitting of the Cf(III) compared to the Dy(III). They calculated a ligand-field strength for $Cf(DPA)_3.H_2O$ of 1632 cm^{-1} considering a spin-orbit coupling constant of 3536 cm^{-1}. This is clearly out of the Bleaney's assumptions since the crystal-field interaction is supposed to be lower than *kT*.

The magnetic susceptibility anisotropies reflected in the particularly high C_a^D term for U(III), Np(III) and Cm(III) would suggest variations of the crystal field parameter induced by the ethyl-DPA ligand along the An(III) series. This contrasts with the constant and low value of An(III) crystal field ($A_0^2\langle r^2\rangle$ = 52 ± 1 cm^{-1}) deduced from temperature experiments and make inconsistent the use of Bleaney's equation to An(III) cations.

The temperature dependence of C_a^D has been calculated in the 250 – 350 K range and decomposed according to T^{-2} and T^{-3}. From the $T^2C_a^D$ = *f(T^{-1})* and $T^2C_a^D$ = *f(T^{-1})* plots (**Figures S16**) Np(III) and Cf(III) present clearly a good C_a^D correlation with a T^{-3} law while for all the other An(III) SO-CASPT2 calculations exhibit a better agreements with a T^{-2} law. Nevertheless, considering a $T^2C_a^D$=*f(T^{-1})* behavior for all studied An(III), τ_2/T values (**Table 14**) deduced from slope (C_a'') and intercept (C_a') ratios present negative values which are consistent with the experimental ones (**Table 8**) for Pu(III), Am(III), Cm(III) and Cf(III). The small τ_2/T value for the Cm(III) seems to confirm the only T^{-2} temperature dependence of the dipolar contribution as assumed in Bleaney's equation.

Table 14. τ_2/T parameter (T=300K) calculated for $[An(DPA)_3]^{3-}$ complexes depicting the temperature deviations of the T^{-2} dipolar contributions in Bleaney's equation.

U(III)	Np(III)	Pu(III)	Am(III)	Cm(III)	Cf(III)
0.30	-0.29	-0.81	-0.63	0.01	-0.67

Conclusions

The study of paramagnetic shifts in $[Ln/An(ethyl\text{-}DPA)_3]^{3-}$ complexes pointed out the difficulties of achieving a good separation of the different contributions in the framework of Bleaney's equation. Nevertheless, the association of different analysis methods permitted to check the isostructurality of the complexes and the constancy of parameters F_i and $A_2^0\langle r^2\rangle$ along the series. The structures of the complexes were resolved by XRD and EXAFS.

The separation methods using one or three nuclei have been applied to the lanthanide complexes in order to determine the F_i and $A_0^2\langle r^2\rangle$ parameters. A geometry variation of these complexes was detected for the heavy lanthanide cations by the ^{13}C paramagnetic shift study (^{13}C nuclei being more sensitive than ^1H to environment change due to the p orbitals). This variation identified as a twisting of the pyridine ring relative to the main axis of the magnetic susceptibility, contrasts to a previous interpretation suggesting a quick flip-flop of the cycle.[5a] However twisting moves are fast at NMR timescale in solution leading to geometric information averaged into the paramagnetic chemical shift $(\delta_{para})_{i,a}$ that evolves along the Ln(III) series. This might be an explanation to the break in the *Fi* value observed between Eu(III) and Tb(III). But on the other hand, F_i can be determined independently from geometry as the $\langle S_z\rangle_a/C_a^D$ ratio and the break cannot be explained by Bleaney's theory.

The temperature dependence of $\langle S_z\rangle_a$ and C_a^D determined experimentally and from quantum chemical calculations are in agreement. They are well fitted by T^{-3}, T^{-2} and T^{-2}, T^{-1} contributions for the dipolar and contact terms respectively. These extra contributions bring a better description of the Ln(III) induced paramagnetic shifts and are particularly required for the first half of the Ln(III) series. However there are some deviations between the experimental and theoretical for C_a^D: it might be due to the simplification by Bleaney of the χ anisotropy to only one crystal field parameter, namely $A_0^2\langle r^2\rangle$.

At first sight, ^1H paramagnetic chemical shifts of $[An(ethyl\text{-}DPA)_3]^{3-}$ complexes, An(III) (from Pu(III) to Cf(III)) exhibit larger contact contributions than Ln(III) and the three nuclei method is in favor of one single set of F_i parameters for the whole actinide series, conversely to Ln(III). Similarly to Ln(III), the temperature behavior of the contact and dipolar contributions exhibit deviations from T^{-1} and T^{-2} with T^{-2} and T^{-3} extra terms required for the light An(III). However for some An(III) these extra terms deviate from temperature dependences of $\langle S_z\rangle_a$ and C_a^D obtained by SO-CASPT2 calculations. Surprisingly the crystal field parameter $A_0^2\langle r^2\rangle$ is found as weak as for the Ln(III) while the 5*f* orbitals of An are expected to interact more with their environment than the 4*f* of the Ln. Contrary to the statements of Bleaney's equation, F_i parameters are not constant along the An(III) series. For the first time $\langle S_z\rangle_a$ and C_a^D have been calculated for An(III) cations by quantum chemistry calculations and normalized to Gd(III) and Dy(III) respectively. Experimental $\langle S_z\rangle_a$ and C_a^D values account for experimental temperature dependences but the C_a^D values differ from theoretical values deduced from *ab-initio* calculations even more than the for Ln(III).

It was anticipated that the application of Bleaney's theory to 5*f* elements would encounter some difficulties in the description of the paramagnetic chemical shifts $(\delta_{para})_{i,a}$ because of the larger interaction of the 5*f* orbitals with the ligands. This experimental and theoretical study shows that F_i values are not constant along the series and that the An(III) crystal field parameter is the same as the Ln(III) one while the splitting of the *J* ground term of the free ion is about three times larger in An(III) than in Ln(III) (see **Tables S16** and **S17**). Consequently it appears that Bleaney's parameters are hardly applicable to An(III) complexes and consequently $\langle S_z\rangle_a$ and C_a^D parameters cannot be representative and used as covalence scale between Ln(III) and An(III).

Experimental Section

Caution! *^{239}Pu, ^{241}Am, ^{244}Cm and ^{249}Cf are highly radioactive isotopes and have to be handled in dedicated facilities with appropriate equipment for radioactive materials. Isotopy details of the actinide ions used for NMR and EXAFS analysis are U (99,29% 238; 0,71% 235), Np (mainly 237), Pu (0,082% 238; 81,498% 239; 17,296% 240; 0,747% 241 and 0,377% 242), Am (98,7% 241 and 1,3% 243), Cm (0,90% 243; 72,17% 244; 12,68% 245; 13,09% 246; 0,59% 247 and 0,57% 248) and Cf (mainly 249).*

Synthesis of solids precursors and ligand:

The hexachloride compounds of actinide and lanthanide(III) (Cs_2NaMCl_6) were prepared according to a protocol described by Morss *et al.* in 1970.[34] Ethyl-DPA ligand was synthesized in the lab according to the protocol described by Shelkov. [35] Ethyl-DPA purity was checked by ^1H NMR.

^1H NMR (400 MHz, DMSO-d6) : δ (ppm) 7.76 (s, 2H, H_3), 2.65 (q, J = 7.58 Hz, 2H, H_5), 1.18 (t, J = 7.58 Hz, 3H, H_6).

Preparation of $An^{III}/Ln^{III}(DPA)_3^{3-}$ solid compounds:

The solution of ligand was prepared by dissolving corresponding amounts of 2,6-pyridine dicarboxylic acid (H_2PDA) and imidazole (Im) with molar ratio H_2PDA:Im 1:2 in water, so that concentration of $(Him)_2PDA$ being about 0.5 M.. Aqueous solutions of metal (M) nitrates concentration (0.05M<[M]<1.0M) were used with the exception of Pu complex. Storage at ambient temperature of aqueous solution prepared by addition of aqueous solution of metal nitrates into 0.5 M $(HIm)_2PDA$ solution up to molar ratio M:$(Him)_2PDA$ of about 1:4 leads to formation of large elongated prismatic crystals which colors meet the color of aqueous solution of corresponding metal nitrate, with the exception of Ce(III) complex which is bright yellow. In the case of Pu(III) the ~1 ml of Pu amalgam with Pu content of about 20-30 mg was placed in ~0.2 ml of aqueous solution of 0.1 M $(Him)_2PDA$ and sealed in glass ampoule. Very quickly large dark almost black crystals become to growth at ambient temperature. Once the crystals were removed from solution, they remain stable as dry solid at air storage.

XRD

X-ray diffraction experiments were carried out on a Bruker KAPPA APEX II autodiffractometer (MoKα radiation, graphite monochromator) at 100 K. The crystals were sealed in glass capillaries. For Am compound, first 20 frames were remeasured at the end of the experiment to check for possible self-radiolysis. Average loss of diffraction intensities was less than 2%. Data reduction was made using SAINT-Plus program. Absorption correction was made using SADABS program. The structures were solved by direct method (SHELXS97) and refined on F2 with the full-matrix least-squares procedure (SHELXL97) using all reflections. The

H-atoms of PDA^{2-} anions and imidazolium cations were placed in geometrically calculated positions. The H atoms of crystallization water molecules were located from difference Fourier maps and refined with restrained O-H distances and H-O-H angles. All the compounds are isostructural and crystallize in triclinic space group P-1.

Preparation of An/Ln(ethyl-DPA)$_3^{3-}$ complexes:

All preparation and experiments were carried out under air except for Pu(III) for which preparation and analysis was performed under argon using standard vacuum-line techniques.

The lanthanide and actinide complexes were synthesized from a 1:8 mixture of solid precursor (Cs_2NaMCl_6) and ethyl-DPA respectively in DMSO. The mixture was stirred for 15 min at room temperature and the dipicolinate and CsCl excess was removed by centrifugation.

NMR

^{1}H NMR spectra were recorded using 400 MHz Fourier transform spectrometers, Agilent DD2, set up for the study of radioactive samples. BMS were collected at every 5°C step in several temperature ranges.

EXAFS

The EXAFS measurements were carried out on the MARS beamline of the SOLEIL synchrotron facility. The optics consists essentially of a double-crystal monochromator which is used to select the incident energy of the X-ray beam. Horizontal and vertical focalization is also provided by a monochromator and by two reflecting mirrors which are used to eliminate the harmonic energy. All experiments were performed at room temperature (≈25°C) and the spectra were collected in transmission mode. In the EXAFS region, data were collected at a constant step (0.05 $Å^{-1}$). Energy calibration was carried out by using K-edge of yttrium to 17038 eV. EXAFS oscillations were extracted after normalization with the Athena software.[36] A square function was applied to the Fourier transform to obtain the pseudo-radial distribution function. The EXAFS data were then adjusted with the Artemis software[36] using the theoretical functions of phase and amplitude calculated with the FEFF8.4 code[19] from the single crystal XRD data. Adjustments have been performed on ΔE0, Amp, σ_2, ΔR parameters corresponding to the offset to k = 0, the amplitude of the oscillations, the Debye - Waller parameter and the distance variations respectively. The coordination number N has been fixed with respect to crystallographic data.

Quantum chemical calculations

Complexes $[Ln(DPA)_3]^{3-}$ and $[An(DPA)_3]^{3-}$ have been described by SO-CASSCF and SO-CASPT2 methods respectively using MOLCAS8.0 suite of program.[37] using the crystallographic geometry for all complexes except for Cm(III) and Cf(III) complexes where optimized geometries. In the case of Am(III) and Pu(III), calculations with optimized geometries were compared to the crystallographic ones and were found to be in very good agreement. All atoms are described with all electron basis sets ANO-RCC.[38] Ln and An atoms with QZP and other atoms with TZP. In the case of Cf, ANO-DK3 augmented to TZP were used [37] The active space consists of n electrons in the 7 *f* orbitals for an atom of configuration $4/5f^n$. First, a multi-state CASSCF (Complete Active Space Self Consistent Field) calculation is performed.[39] For An(III) complexes, dynamical correlation is calculated using MS-CASPT2 method.[40] Spin-orbit coupling is evaluated as a state interaction between CASSCF or MS-CASPT2 wave functions by the RASSI (Restricted Active Space State Interaction) method.[41] Spin-orbit integrals are evaluated within AMFI approximation.[42] For Ln(III) complexes, all the states with the largest spin were taken into account. For Am(III), 7 septets and 31 quintets , for Pu(III), 21 sextets, 48 quartets and 31 doublets, for Cm(III), 1 octet, 37 sextets and 16 quartets, and for Cf(III), 21 sextets and 63 quartets are taken into account in the state interaction The calculation of all the properties is implemented in a local program. Magnetic susceptibility is calculated according to S. Vancoillie *et al.* [43] and $\langle S_z \rangle$ along the same scheme switching off the orbital contribution.

Acknowledgements

We are grateful to the support from ANR under the convention N°ANR-17-CE06-0010. We thank Pr J.F. Desreux for interesting and fruitful discussions all along this project.

Keywords: actinide(III) • lanthanide(III) • NMR paramagnetic shift • dipicolinate • EXAFS • single-crystal XRD

[1] a) J. G. Brennan, J. C. Green, C. M. Redfern, *Journal of the American Chemical Society* **1989**, *111*, 2373-2377; b) R. E. Cramer, R. B. Maynard, J. C. Paw, J. W. Gilje, *Organometallics* **1983**, *2*, 1336-1340; c) A. J. Gaunt, S. D. Reilly, A. E. Enriquez, B. L. Scott, J. A. Ibers, P. Sekar, K. I. M. Ingram, N. Kaltsoyannis, M. P. Neu, *Inorganic Chemistry* **2008**, *47*, 29-41; d) K. I. M. Ingram, M. J. Tassell, A. J. Gaunt, N. Kaltsoyannis, *Inorganic Chemistry* **2008**, *47*, 7824-7833; e) N. Kaltsoyannis, *Inorganic Chemistry* **2000**, *39*, 6009-6017; f) S. A. Kozimor, P. Yang, E. R. Batista, K. S. Boland, C. J. Burns, D. L. Clark, S. D. Conradson, R. L. Martin, M. P. Wilkerson, L. E. Wolfsberg, *Journal of the American Chemical Society* **2009**, *131*, 12125-12136; g) M. Roger, L. Belkhiri, T. Arliguie, P. Thuery, A. Boucekkine, M. Ephritikhine, *Organometallics* **2008**, *27*, 33-42.

[2] a) F. Inagaki, T. Miyazawa, *Progress in Nuclear Magnetic Resonance Spectroscopy* **1980**, *14*, 67-111; b) J. A. Peters, J. Huskens, D. J. Raber, *Progress in Nuclear Magnetic Resonance Spectroscopy* **1996**, *28*, 283-350.

[3] a) S. P. Babailov, Y. G. Krieger, *J Struct Chem* **1998**, *39*, 580-593; b) I. Bertini, C. Luchinat, *Coord. Chem. Rev.* **1996**, *150*, 185-220; c) J. F. Desreux, C. N. Reilley, *Journal of the American Chemical Society* **1976**, *98*, 2105-2109; d) C. F. G. C. Geraldes, A. D. Sherry, G. E. Kiefer, *Journal of Magnetic Resonance* **1992**, *97*, 290-304; e) C. N. Reilley, B. W. Good, *Analytical Chemistry* **1975**, *47*, 2110-2116; f) C. N. Reilley, B. W. Good, R. D. Allendoerfer, *Analytical Chemistry* **1976**, *48*, 1446-1458; g) A. G. Martynov, Y. G. Gorbunova, A. Y. Tsivadze, *Dalton Transactions* **2011**, *40*, 7165-7171; h) A. D. Sherry, M. Singh, C. Geraldes, *Journal of Magnetic Resonance* **1986**, *66*, 511-524.

[4] a) K. Tori, Y. Yoshimura, M. Kainosho, K. Ajisaka, *Tetrahedron Letters* **1973**, *14*, 3127-3130; b) D. J. Chadwick, D. H. Williams, *Journal of the Chemical Society, Perkin Transactions 2* **1974**, 1202-1206.

[5] a) N. Ouali, B. Bocquet, S. Rigault, P. Y. Morgantini, J. Weber, C. Piguet, *Inorganic Chemistry* **2002**, *41*, 1436-1445; b) S. Rigault, C. Piguet, J.-C. G. Bunzli, *Journal of the Chemical Society, Dalton Transactions* **2000**, 2045-2053.

[6] a) B. Bleaney, *Journal of Magnetic Resonance* **1972**, *8*, 91-100; b) B. Bleaney, R. J. P. Williams, A. V. Xavier, R. B. Martin, B. A. Levine, C. M. Dobson, *Journal of the Chemical Society-Chemical Communications* **1972**, 791-793.

[7] A. A. Pinkerton, M. Rossier, S. Spiliadis, *Journal of Magnetic Resonance (1969)* **1985**, *64*, 420-425.

[8] a) G. T. P. Charnock, I. Kuprov, *Phys. Chem. Chem. Phys.* **2014**, *16*, 20184-20189; b) A. M. Funk, K.-L. N. A. Finney, P. Harvey, A. M. Kenwright, E. R. Neil, N. J. Rogers, P. Kanthi Senanayake, D. Parker, *Chem. Sci.* **2015**, *6*, 1655-1662; c) O. A. Blackburn, R. M. Edkins, S. Faulkner, A. M. Kenwright, D. Parker, N. J. Rogers, S. Shuvaev, *Dalton Trans.* **2016**, *45*, 6782-6800; d) E. A. Suturina, I. Kuprov, *Physical Chemistry Chemical Physics* **2016**, *18*, 26412-26422.

[9] I. Bertini, M. B. L. Janik, Y.-M. Lee, C. Luchinat, A. Rosato, *Journal of the American Chemical Society* **2001**, *123*, 4181-4188.

[10] a) V. S. Mironov, Y. G. Galyametdinov, A. Ceulemans, C. Görller-Walrand, K. Binnemans, *The Journal of Chemical Physics* **2002**, *116*, 4673-4685; b) S. Rigault, C. Piguet, J.-C. G. Bunzli, *J. Chem. Soc., Dalton Trans.* **2000**, 2045-2053.

[11] *Coordination Chemistry Reviews* **1996**, *150*, 111-130.

[12] a) F. Gendron, K. Sharkas, J. Autschbach, *J. Phys. Chem. Lett.* **2015**, *6*, 2183-2188; b) J. Vaara, S. A. Rouf, J. Mareš, *J. Chem. Theory Comput.* **2015**, *11*, 4840-4849; c) W. Van den Heuvel, A. Soncini, *Phys. Rev. Lett.* **2012**, *109*, 073001-073001; d) A. Soncini, W. Van den Heuvel, *The Journal of Chemical Physics* **2013**, *138*, 021103-021103.

[13] J. Reuben, D. Fiat, *Journal of Chemical Physics* **1969**, *51*, 4909-4917.

[14] a) C. Geraldes, S. R. Zhang, C. Platas, T. Rodriguez-Blas, A. de Blas, A. D. Sherry, *Journal of Alloys and Compounds* **2001**, *323*, 824-827; b) C. Platas, F. Avecilla, A. de Blas, C. Geraldes, T. Rodriguez-Blas, H. Adams, J. Mahia, *Inorganic Chemistry* **1999**, *38*, 3190-3199; c) J. M. Ren, A. D. Sherry, *Journal of Magnetic Resonance Series B* **1996**, *111*, 178-182.

[15] S. K. Cary, M. Vasiliu, R. E. Baumbach, J. T. Stritzinger, T. D. Green, K. Diefenbach, J. N. Cross, K. L. Knappenberger, G. Liu, M. A. Silver, A. E. DePrince, M. J. Polinski, S. M. Van Cleve, J. H. House, N. Kikugawa, A. Gallagher, A. A. Arico, D. A. Dixon, T. E. Albrecht-Schmitt, *Nat Commun* **2015**, *6*, 1-8.

[16] a) A. M. Fedosseev, M. S. Grigoriev, N. A. Budantseva, D. Guillaumont, C. Le Naour, E. Simoni, C. Den Auwer, P. Moisy, *Comptes Rendus*

ACCEPTED MANUSCRIPT

Chimie **2010**, *13*, 839-848; b) N. L. Banik, M. A. Denecke, A. Geist, G. Modolo, P. J. Panak, J. Rothe, *Inorganic Chemistry Communications* **2013**, *29*, 172-174; c) M. A. Denecke, P. J. Panak, F. Burdet, M. Weigl, A. Geist, R. Klenze, M. Mazzanti, K. Gompper, *Comptes Rendus Chimie* **2007**, *10*, 872-882; d) L. Karmazin, M. Mazzanti, J. P. Bezombes, C. Gateau, J. Pecaut, *Inorganic Chemistry* **2004**, *43*, 5147-5158; e) M. Mazzanti, R. L. Wietzke, J. Pecaut, J. M. Latour, P. Maldivi, M. Remy, *Inorganic Chemistry* **2002**, *41*, 2389-2399.

[17] P. D'Angelo, A. Zitolo, V. Migliorati, G. Chillemi, M. Duvail, P. Vitorge, S. Abadie, R. Spezia, *Inorganic Chemistry* **2011**, *50*, 4572-4579.

[18] F. H. David, B. Fourest, *New Journal of Chemistry* **1997**, *21*, 167-176.

[19] J. J. Rehr, R. C. Albers, *Reviews of Modern Physics* **2000**, *72*, 621-654.

[20] a) C. Adam, B. B. Beele, A. Geist, U. Mullich, P. Kaden, P. J. Panak, *Chem. Sci.* **2015**, *6*, 1548-1561; b) C. Adam, P. Kaden, B. B. Beele, U. Mullich, S. Trumm, A. Geist, P. J. Panak, M. A. Denecke, *Dalton Trans.* **2013**, *42*, 14068-14074.

[21] C. N. Reilley, B. W. Good, R. D. Allendoerfer, *Anal. Chem.* **1976**, *48*, 1446-1458.

[22] B. M. Alsaadi, F. J. C. Rossotti, R. J. P. Williams, *Journal of the Chemical Society-Dalton Transactions* **1980**, 597-602.

[23] C. F. G. C. Geraldes, S. Zhang, A. D. Sherry, *Inorg. Chim. Acta* **2004**, *357*, 381-395.

[24] R. J. Kurland, B. R. McGarvey, *Journal of Magnetic Resonance* **1970**, *2*, 286-301.

[25] B. R. McGarvey, *Journal of Magnetic Resonance* **1979**, *33*, 445-455.

[26] G. N. LaMar, W. D. Horrocks, R. H. Holm, *NMR of Paramagnetic Molecules: Principles and Applications*, Elsevier Science, London, **1973**.

[27] M. Hiller, S. Krieg, N. Ishikawa, M. Enders, *Inorganic Chemistry* **2017**, *56*, 15285-15294.

[28] I. Bertini, C. Luchinat, G. Parigi, *Prog. Nucl. Magn. Reson. Spectrosc.* **2002**, *40*, 249-273.

[29] R. Golding, M. Halton, *Australian Journal of Chemistry* **1972**, *25*, 2577-2581.

[30] M. Autillo, L. Guerin, H. Bolvin, P. Moisy, C. Berthon, *Phys. Chem. Chem. Phys.* **2016**, *18*, 6515-6525.

[31] E. A. Suturina, K. Mason, C. F. G. C. Geraldes, I. Kuprov, D. Parker, *Angewandte Chemie International Edition* **2017**, *56*, 12215-12218.

[32] K. Mason, N. J. Rogers, E. A. Suturina, I. Kuprov, J. A. Aguilar, A. S. Batsanov, D. S. Yufit, D. Parker, *Inorganic Chemistry* **2017**, *56*, 4028-4038.

[33] M. Vonci, K. Mason, E. A. Suturina, A. T. Frawley, S. G. Worswick, I. Kuprov, D. Parker, E. J. L. McInnes, N. F. Chilton, *J. Am. Chem. Soc.* **2017**, *139*, 14166-14172.

[34] L. R. Morss, M. Siegal, L. Stenger, Edelstei.N, *Inorganic Chemistry* **1970**, *9*, 1771-1775.

[35] R. Shelkov, A. Melman, *European Journal of Organic Chemistry* **2005**, *2005*, 1397-1401.

[36] B. Ravel, M. Newville, *Journal of Synchrotron Radiation* **2005**, *12*, 537-541.

[37] F. Aquilante, L. De Vico, N. Ferre, G. Ghigo, P.-A. Malmqvist, P. Neograd y, T. B. Pedersen, M. Pitonak, M. Reiher, B. O. Roos, L. Serrano-Andres, M. Urban, V. Veryazov, R. Lindh, *Journal of Computational Chemistry* **2010**, *31*, 224-247.

[38] a) B. O. Roos, R. Lindh, P. A. Malmqvist, V. Veryazov, P. O. Widmark, *Journal of Physical Chemistry A* **2004**, *108*, 2851-2858; b) B. O. Roos, R. Lindh, P.-A. Malmqvist, V. Veryazov, P.-O. Widmark, A. C. Borin, *Journal of Physical Chemistry A* **2008**, *112*, 11431-11435.

[39] B. O. Roos, P. R. Taylor, P. E. M. Siegbahn, *Chemical Physics* **1980**, *48*, 157-173.

[40] K. Andersson, P. A. Malmqvist, B. O. Roos, A. J. Sadlej, K. Wolinski, *Journal of Physical Chemistry* **1990**, *94*, 5483-5488.

[41] P. A. Malmqvist, B. O. Roos, B. Schimmelpfennig, *Chemical Physics Letters* **2002**, *357*, 230-240.

[42] B. A. Hess, C. M. Marian, U. Wahlgren, O. Gropen, *Chemical Physics Letters* **1996**, *251*, 365-371.

[43] S. Vancoillie, L. Rulíšek, F. Neese, K. Pierloot, *The Journal of Physical Chemistry A* **2009**, *113*, 6149-6157.

WILEY-VCH

WILEY-VCH

Entry for the Table of Contents (Please choose one layout)

FULL PAPER

Is Bleaney's equation for pNMR shifts of Ln(III) valid for An(III) complexes ?

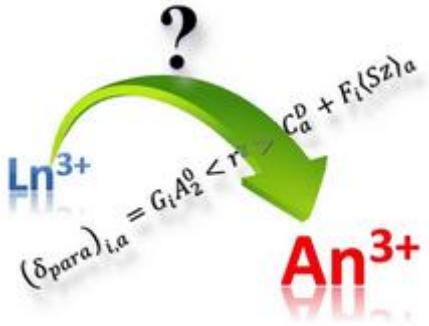

M. Autillo, L. Guerin, T. Dumas, M. S. Grigoriev, A. M. Fedoseev, S. Cammelli, P. L. Solari, D. Guillaumont, P. Guilbaud, P. Moisy, H. Bolvin, and C. Berthon**

Page No. – Page No.

Insight of the metal-ligand interaction in f elements complexes by paramagnetic NMR spectroscopy.

WILEY-VCH